Transcriptome Analysis of *Solanum Tuberosum* Genotype RH89-039-16 in Response to Chitosan

Philipp Lemke, Bruno M. Moerschbacher* and Ratna Singh*

Institute for Biology and Biotechnology of Plants, University of Münster, Münster, Germany

Potato (*Solanum tuberosum* L.) is the worldwide most important nongrain crop after wheat, rice, and maize. The autotetraploidy of the modern commercial potato makes breeding of new resistant and high-yielding cultivars challenging due to complicated and time-consuming identification and selection processes of desired crop features. On the other hand, plant protection of existing cultivars using conventional synthetic pesticides is increasingly restricted due to safety issues for both consumers and the environment. Chitosan is known to display antimicrobial activity against a broad range of plant pathogens and shows the ability to trigger resistance in plants by elicitation of defense responses. As chitosan is a renewable, biodegradable and nontoxic compound, it is considered as a promising next-generation plant-protecting agent. However, the molecular and cellular modes of action of chitosan treatment are not yet understood. In this study, transcriptional changes in chitosan-treated potato leaves were investigated *via* RNA sequencing. Leaves treated with a well-defined chitosan polymer at low concentration were harvested 2 and 5 h after treatment and their expression profile was compared against water-treated control plants. We observed 32 differentially expressed genes (fold change ≥ 1; p-value ≤ 0.05) 2 h after treatment and 83 differentially expressed genes 5 h after treatment. Enrichment analysis mainly revealed gene modulation associated with electron transfer chains in chloroplasts and mitochondria, accompanied by the upregulation of only a very limited number of genes directly related to defense. As chitosan positively influences plant growth, yield, and resistance, we conclude that activation of electron transfer might result in the crosstalk of different organelles *via* redox signals to activate immune responses in preparation for pathogen attack, concomitantly resulting in a generally improved metabolic state, fostering plant growth and development. This conclusion is supported by the rapid and transient production of reactive oxygen species in a typical oxidative burst in the potato leaves upon chitosan treatment. This study furthers our knowledge on the mode of action of chitosan as a plant-protecting agent, as a prerequisite for improving its ability to replace or reduce the use of less environmentally friendly agro-chemicals.

Keywords: transcriptome analysis, RNAseq, potato, chitosan, defense, photosynthesis

INTRODUCTION

Feeding an increasing world population remains one of the most important global tasks. In spite of the ongoing optimization of crops by modern plant breeding, agricultural production will be insufficient to nourish an expected ten billion people in 2050 unless agricultural practices are further improved. The situation is further exacerbated by a decline of farmland as a consequence of climate change and urbanization. With a global production of over 388 million tons in 2018 (FAOSTAT, www.fao.org), potato (*Solanum tuberosum* L.) is the world's most important nongrain crop, exceeded only by the three top cereals, maize, wheat, and rice (Zaheer and Akhtar, 2016). Especially due to its high yield and nutritive composition including starch, vitamins, and antioxidants (Burlingame et al., 2009), potato is a crucial element in food security, particularly in developing countries of South America, Africa, and Asia (Scott and Suarez, 2012). Its autotetraploid and heterozygous nature, however, impedes the selection of desirable plant characteristics after crossing and is thus a challenge for modern breeding (Muthoni et al., 2015). To facilitate conventional breeding as well as genetic studies, diploid variants are used to overcome the complicated and difficult to trace heredity, and the homozygous, doubled-monoploid potato variant DM1-3 516 R44 was eventually used to sequence the potato genome in 2011 (Xu et al., 2011). This genome sequence was subsequently used to integrate data from the heterozygous diploid variant RH89-039-16, which more closely resembles commercial potato cultivars (Xu et al., 2011), hence opening new paths to investigate potato genomics and transcriptomics and thereby noticeably improving its breeding, cultivation, and protection.

In parallel to these efforts aiming to genetically improve crop cultivars, plant protection measures are essential to ensure crop yields and quality. These are not only subject to varying biotic and abiotic stress pressures, but also to changing legal regulations and consumer preferences. Increasing stress conditions due to climate change and increasing demand for healthy, residue-free, and sustainably produced crops, accompanied by a low acceptance of genetically engineered crop plants, call for the development of alternative or, rather, complementing plant production practices. Ideally, novel agro-chemical or agro-biological compounds should combine antimicrobial as well as plant-strengthening activities and simultaneously avoid environmental burdens. One of the most promising candidates for such an agrobiologic is chitosan. Chitosans are partially or fully *N*-deacetylated derivatives of chitin (poly-β-(1-4)-*N*-acetyl-D-glucosamine), the most abundant aminosugar biopolymer on earth. Chitin is naturally found, e.g., in the exoskeletons of arthropods and cell walls of fungi and yeast, acting as a structural polysaccharide (Rinaudo, 2006). Chitin is nontoxic, biodegradable, and an abundant renewable resource, but its crystallinity and, hence, insolubility severely limit its usability in agriculture. In contrast, chitosans, which are protonated and, hence, polycationic at slightly acidic pH values, are more easily soluble. Their solubility is strongly dependent on their degree of polymerization (DP) and, even more prominently, on their

fraction of acetylation (FA), i.e., the mole fraction of anhydro-2-acetamido-2-deoxy-D-glucose units (Roberts, 2008). Furthermore, both DP and FA strongly affect the bioactivity of chitosans (Cord-Landwehr et al., 2020; Wattjes et al., 2020). Low FA chitosans have the highest antimicrobial activities (Omura et al., 2003; Gueddari and Moerschbacher, 2004; Younes et al., 2014), as reported against a broad range of plant pathogens, including oomycetes (Sharp, 2013), bacteria, fungi, viruses (Kulikov et al., 2006), and even herbivore insects (Rabea et al., 2005). On the other hand, intermediate to high FA chitosans seem to be best to elicit defense reactions in plants (Vander et al., 1998; Gueddari and Moerschbacher, 2004; Nietzel et al., 2018), e.g., triggering chitinase activity (Katiyar et al., 2014) as well as the biosynthesis of phenolics and phytoalexins (Bautista-Baños et al., 2006). While the antimicrobial activity of chitosans appears to depend on their polycationic nature favoring electrostatic interactions with negatively charged cell surfaces, their effect on plants is believed to be receptor mediated (Gueddari and Moerschbacher, 2004). In plants, chitosans most likely act as a pathogen or microbe associated molecular patterns (PAMP/MAMP) which are recognized through pattern recognition receptors (PRR) such as the chitin receptor CERK1 in *Arabidopsis* or CEBiP in rice (Iriti and Faoro, 2009). This so called PAMP-triggered immunity (PTI) is a well-studied and important defense system in plants which involves a number of signal transduction cascades, eventually resulting in the synthesis of proteins, reactive oxygen species (ROS), secondary metabolites, and phytohormones, to name just a few (Jones and Dangl, 2006; Miller et al., 2017).

In spite of the well-documented protective effects of chitosans in different plant species and against different pathogens (Hadrami et al., 2010), still surprisingly little evidence is provided concerning their actual mode of action, especially on a molecular level. Investigations regarding the effect of chitin oligomers on plants on a molecular level started in the early 2000s with microarray studies on *Arabidopsis* seedlings (Ramonell et al., 2002) and rice cell cultures (Akimoto-Tomiyama et al., 2003). Microarray studies were further pursued with chitosan oligomers on oilseed rape plants (Yin et al., 2006), *Arabidopsis* seedlings (Povero et al., 2011) and whole *Arabidopsis* plants (Jia et al., 2016). Only recently, first transcriptome studies using an RNAseq approach have been reported in chitosan-treated strawberry (Landi et al., 2017) and avocado (Xoca-Orozco et al., 2017) fruits. While a protective effect of chitosan treatment on potato, e.g., against *Phytophthora infestans* (O'Herlihy et al., 2003; Chang and Kim, 2012; Ippólito et al., 2017) or potato virus X (Chirkov et al., 2001) has been described, no such transcriptomic study has been conducted in potato yet. However, several transcriptome analyses on potato have been published, e.g., describing gene expression under drought stress (Gong et al., 2015) and other abiotic and biotic stresses (Massa et al., 2013), mostly based on the reference data for the potato transcriptome by Massa et al. (2011). Here, we report on a whole transcriptome analysis of potato genotype RH89-039-16 following treatment with a well-defined chitosan.

MATERIAL AND METHODS

Chitosan

The chitosan used in this study was derived from shrimp shell α-chitin and received from Mahtani Chitosan Pvt. Ltd. (Veraval, India). It had an average FA of 0.2 as determined *via* proton nuclear magnetic resonance (^{1}H-NMR) (Hirai et al., 1991; Lavertu et al., 2003), and a weight average molecular weight (Mw) of 87 kDa (DPw 515), as determined using size exclusion chromatography coupled to refractive index detection and multiangle laser light scattering (HPSEC-RI-MALLS) (Schatz et al., 2003). The dispersity Đ of the DP was determined as $Đ_{DP}$ = Mw/Mn = 2. Chitosan solutions were obtained by dispersing chitosan powder in distilled water and solubilization with a 5% molar excess of acetic acid relative to the free amino groups in the chitosan used.

Potato Cultivation and Leaf Treatment

Potato plants obtained from tubers were cultivated in an environmental chamber with constant temperatures under long-day conditions (16/8 h photoperiod, 24/18°C). One day before treatment, mature leaves were detached from fully developed side shoots and collected on petri dishes containing water agar (0.05% agar in distilled water). The petri dishes were closed and incubated in the environmental chamber for 24 h. This procedure ensured the de-stressing of the leaves overnight after being detached from the plant. For treatment, the abaxial surfaces of the leaves were sprayed with a 0.05% chitosan solution, or with distilled water as a control, until small droplets formed on the leaf surface. Treated leaves were incubated in the environmental chamber again before being frozen in liquid nitrogen 2 and 5 h after treatment. These times were chosen as a result of extensive pretests and quantitative PCR (qPCR) studies using potentially chitosan-triggered genes including WRKY transcription factors and resistance genes, aimed to identify appropriate time points for the transcriptome analysis. This resulted in a total of twelve samples, with two time points, two treatments, and three biological replicates each.

RNA Isolation

To isolate the RNA from the frozen leaves, leaf tissue was ground with mortar and pestle under liquid nitrogen. Extraction of RNA from the leaf powder was done using the innuPREP RNA Mini Kit from Analytik Jena (Jena, Germany). DNA was removed with a provided precolumn which eliminated DNAse digestion. RNA quality and quantity were determined *via* Nanodrop 2000 (Thermo Fisher Scientific, Waltham, Massachusetts, USA) and a Bioanalyzer 2100 (Agilent Technologies, Santa Clara, California, USA) prior to sequencing.

RNA Sequencing

The sequencing library was prepared following the Illumina TruSeq mRNA protocol (https://support.illumina.com/downloads/truseq_stranded_mrna_sample_preparation_guide_15031047.html). The sequencing was conducted with an Illumina HiSeq 3000 (Illumina, San Diego, California, USA) with all 12 samples on one HiSeq lane, resulting in 21-26 million 50-bp-reads per sample. After quality control of the raw sequencing data, all reads were computationally aligned to the potato reference genome PGSC v4.03 (Xu et al., 2011). RNAseq quality control and sequencing procedures were performed by GeneVia Technologies (Tampere, Finland), as described below.

Data Analysis

The analysis was started from raw sequencing data in fastq format. The reference genome and its associated annotation gff file were obtained from a specific potato Ensembl page (ftp://ftp.ensemblgenomes.org/pub/release-46/plants/gtf/solanum_tuberosum).

Quality Control

Quality of the RNAseq reads was inspected using FastQC software (Frenkel, 2009). TrimGalore! (Krueger, 2018) was ran on the reads, with default settings.

Read Alignments and Read Counts

RNAseq reads were aligned to *Solanum tuberosum* reference genome Soltub 3.0 using STAR aligner, version 2.5.2 (Dobin et al., 2013). Gene-level read counts were obtained simultaneously with the alignment process. For visual exploration of the data, the obtained read counts were normalized using regularized log transformation function of DESeq2 R package (Love et al., 2014), which transforms the count data to the log_2 scale in a way that minimizes differences between samples for rows with small counts and also normalizes the data with respect to library size. A visual inspection of the samples using principal component analysis (PCA) and a Pearson's correlation heatmap was followed by combining the technical replicates of each sample by averaging their gene counts for subsequent analysis steps.

Differentially Expressed Genes

Data normalization and differential expression analysis were performed using R package DESeq2 (Love et al., 2014). The data was divided per comparison into four groups: CS_5h vs CS_2h, CS_2h vs H$_2$O_2h, H$_2$O_5h vs H$_2$O_2h and CS_5h vs H$_2$O_5h. For each of these, pairedness was included in the design matrices as shown in **Supplementary Table 1**. Heatmaps and volcano plots of the differentially expressed genes were created using pheatmap (Kolde, 2019) and an in-house volcano-visualization function, based on ggplot2 (Wickham, 2011), respectively. Furthermore, a heatmap only including genes upregulated both 2 and 5 h after treatment was created using the iDEP (integrated Differential Expression and Pathway analysis) webtool (http://bioinformatics.sdstate.edu/idep/, accessed on 07.07.2020), comparing gene expression between both times using mean-centered fold change values (Ge et al., 2018). Genes having adjusted p-value <0.05 and absolute log_2 fold change >1 were considered significantly differentially expressed.

Enrichment Analysis

The above groups of differentially expressed genes (DEGs) from each comparison were subjected to enrichment analysis of associations to Gene Ontology (GO) biological process terms.

The enrichment analyses determined whether any GO terms are annotated to a list of specified genes, in this case a list of DEGs, at a frequency greater than what would be expected by chance and calculated a p-value using hypergeometric distribution. A file containing transcript IDs and corresponding protein IDs [http://rsat.eead.csic.es/plants/data/genomes/Solanum_tuberosum.DM.v4.03.PGSC/genome/peptidic_sequences.fasta] was used to associate PGSC transcript IDs to Ensembl protein IDs. A table [http://bioinfo.cau.edu.cn/agriGO/download/item2term_73], displaying correspondence between Ensembl protein IDs and GO entries was used to associate the proteins to GO entries. Finally, the GO terms were associated with their corresponding descriptions using the R GO database (Meurk et al., 2013) and deprecated terms were removed. The conversions returned altogether 13,656 genes with GO term associations. All potato genes with GO annotation were used as background set for the enrichment analysis. The p-values of enrichment analysis were corrected for multiple testing using Benjamini-Hochberg multiple testing adjustment procedure (Hochberg, 1995). GO terms with adjusted p < 0.05 and with at least two genes from a gene group studied were considered significantly enriched. Enrichment analysis was further broadened conducting a cluster-wise enrichment analysis *via* iDEP (integrated Differential Expression and Pathway analysis) webtool (http://bioinformatics.sdstate.edu/idep/, accessed on 07.07.2020) (Ge et al., 2018), including all available gene sets for pathway analysis.

MapMan and Kyoto Encyclopedia of Genes and Genomes Pathway Annotation

MapMan software was used to display the DEG dataset in the context of biological functions and pathways (Thimm et al., 2004; Usadel et al., 2009). To insert the gene expression data, the "Stub_PGSC_DM_v3.4" mapping file for the *S. tuberosum* genome was used which is accessible on the MapMan website. Likewise, the Kyoto Encyclopedia of Genes and Genomes (KEGG) database was used to visualize the DEG dataset and to further illustrate the gene functions (Ogata et al., 1999). The usage of corresponding KEGG pathways were officially granted prior to publication (Kanehisa et al., 2017; Kanehisa et al., 2019).

Validation of DEGs *via* Real-Time qPCR

To validate the gene expression data from the RNAseq, five representative photosynthesis-related DEGs were selected for qPCR studies. qPCR runs were carried out in three independent experiments with triplicates of all samples in each experiment. To minimize natural variation that occurs when using different plants, particularly plants cultivated in different seasons, the same RNA samples were used for qPCR quantification and RNAseq analysis. After extracting the RNA as described above, first strand cDNAs were synthesized from 500 ng of total RNA using PrimeScript RT Master Mix from Takara Bio Inc. (Kusatsu, Shiga, Japan), following the manufacturer's instructions. To conform to qPCR standards, highly specific primers were designed using NCBI Primer Blast (Ye et al., 2012) with melting temperatures (Tm) between 59 and 61°C,

20 bp length and amplicon lengths of 100-200 bp. Self- and cross dimerization of primers was excluded by running the Multiple Primer Analyzer webtool from Thermo Fisher Scientific (Waltham, Massachusetts, USA). As references, housekeeping genes of the elongation factor 1-α (ef1α) and the 18S rRNA were used as previously used in qPCR and RNAseq studies with potato plants (Nicot et al., 2005; Goyer et al., 2015). The primers for the reference genes were designed and approved likewise. All primers are listed in **Supplementary Table 2**. Nontemplate controls were included for each primer pair to exclude false-positive results due to unspecific dye binding. The qPCR cycler was a CFX96 Touch Real-Time PCR Detection System (Bio-Rad Laboratories, Inc., Hercules, California, USA), with initial denaturation at 95°C for 3 min followed by 44 cycles of 95°C for 3 s and 60°C for 20 s. Melting curve analysis was performed from 58 to 95°C, where the temperature increased by 0.5°C every 5 s. The total volume was 10 µl per sample, containing 2.5 µl of cDNA (1:50 dilution from cDNA synthesis samples, i.e., 50 ng), 2.5 µl of a mix of one primer pair (1:250 dilution from 100 µM stock solutions, i.e., 0,4 µM per primer) and 5 µl of KAPA SYBR FAST qPCR Master Mix (Sigma-Aldrich, St. Louis, Missouri, USA). Primer efficiencies were determined using a high-quality cDNA template (as determined *via* Nanodrop) in several factor 10 dilution steps (1:10 to 1:1,000,000), resulting in a standard durve by plotting the log of the cDNA quantity against the cycle threshold value obtained during amplification. An R^2 value > 0.9 was considered as sufficient fitting of the experimental data to the regression line. The primer or amplification efficiency E was eventually calculated from the standard curve slope by the formula $E = 10^{-1/slope}$. Primer efficiencies are given in **Supplementary Table 2**. Analysis of qPCR data was done using the efficiency corrected calculation model described by (Pfaffl, 2001). REST-MCS (relative expression software tool – multiple condition solver) was used to allow the direct comparison of both time points and both treatments in one analysis (Pfaffl, 2002).

Oxidative Burst Assay

To investigate the eliciting activity of chitosan on potato leaves, leaf disks were prepared from fully-grown, mature RH89-039-16 potato leaves that were freshly detached from the plant. Disks were cut *via* gently pressing with a cork borer (Ø 5 mm) on the lamina part of the leaf, avoiding strong veins and the midrib. Each disk was subsequently transferred to a well of a 96 well microtiter plate containing 100 µl of dH2O. The plates were covered with aluminum foil and incubated at room temperature over night to prevent interference of ROS produced after wounding by allowing de-stressing of the freshly cut leaf disks (Bredow et al., 2019). After overnight incubation, the water was replaced by 200 µl of 0.05% chitosan and 0.5 mM of the luminol derivative L-012 (8-amino-5-chloro-7-phenylpyrido[3,4-d]pyridazine- 1,4(2H,3H)dione) (Nishinaka et al., 1993) in 10 mM MOPS/KOH buffer (pH 7.4). H_2O_2 was quantified by a microplate reader measuring the light emission caused by the reaction of H_2O_2 and L-012 (Albert and Fürst, 2017). Chemiluminescence was continuously measured for 5 s per well over a total time of 90 min and is given as relative light units (RLU).

RESULTS

RNAseq Data Analysis

Sample Quality Control and Read Alignment

Total RNA quality tested by Bioanalyzer displayed RIN values ≥8 and 25/18 s ratios between 1.9 and 2.5 for all samples. The quality of all processed samples was also found to be good and consistent, only displaying a slight TruSeq adapter contamination, that was taken care of by a run of TrimGalore!, using default parameters. The alignment statistics are presented in **Supplementary Table 1**. Uniquely mapped alignment rates were consistently above 80% for all samples, except for the CS_5h samples which had >25% of multimapped reads, possibly indicating ribosomal RNA (rRNA) contamination. However, the read counts for differential expression analysis were calculated using only the uniquely mapped reads, and since the total number of reads was high in all samples, this was concluded not to cause problems in differential expression analysis.

Principal Component Analysis and Pearson's Correlation Heatmap

Both PCA and Pearson's correlation coefficient calculations were performed as final methods to ensure data quality. In the PCA including all samples, the two first principal components explained 70.2% of the variance between samples. According to both the visualization of the PCA and Pearson's correlation analysis, the samples did not cluster clearly together by treatment. This may be due to high sample similarity as indicated by the Pearson's correlation values (**Supplementary Figure 1**). **Supplementary Figure 2** presents the visualization of PCA results on samples of one time point but different treatment, which all in all showed that the samples still showed a certain grouping by treatment.

Differentially Expressed Genes

Two hours after treatment, the analysis of differential gene expression yielded a total of 32 DEGs for the comparison chitosan-treated versus water-treated leaves (**Figure 1A**), while 5 h after treatment 83 DEGs were found (**Figure 1B**). Gene expression was clearly in chitosan-treated samples 5 h after treatment in comparison to 2 h after treatment (**Supplementary Figure 3**). **Figure 1** shows the clustering of the DEGs based on their similar expression patterns. In both sample groups (chitosan versus water 2 h after treatment and chitosan versus water 5 h after treatment), the smaller cluster represents the downregulated DEGs while the larger one represents the upregulated DEGs. Consequently, 2 h after chitosan treatment, 28 genes were detected to be upregulated and 4 genes were found to be downregulated, whereas 5 h after chitosan treatment three genes were downregulated and 80 were upregulated. Of all DEGs, 10 were exclusively differentially expressed 2 h after chitosan treatment, while 61 DEGs were exclusively differentially expressed 5 h after chitosan treatment. Twenty-two of all upregulated DEGs were differentially expressed at both time points (**Figure 1C**).

Genes of unknown function are not discussed further as no clear allocation to certain functions or targets are possible.

Interestingly, we observed that chitosan treatment mostly triggered the expression of genes related to electron transport in mitochondria and chloroplasts, including both nuclear- and chloroplast-encoded genes. **Supplementary Table 3** lists all genes mentioned in the following chapters, including their full description and transcriptomic gene IDs. The full lists of differentially expressed genes including their fold changes and p-values are reported in the **raw data** provided.

Chitosan-Triggered Downregulation of Genes Was Limited to Very Few Genes
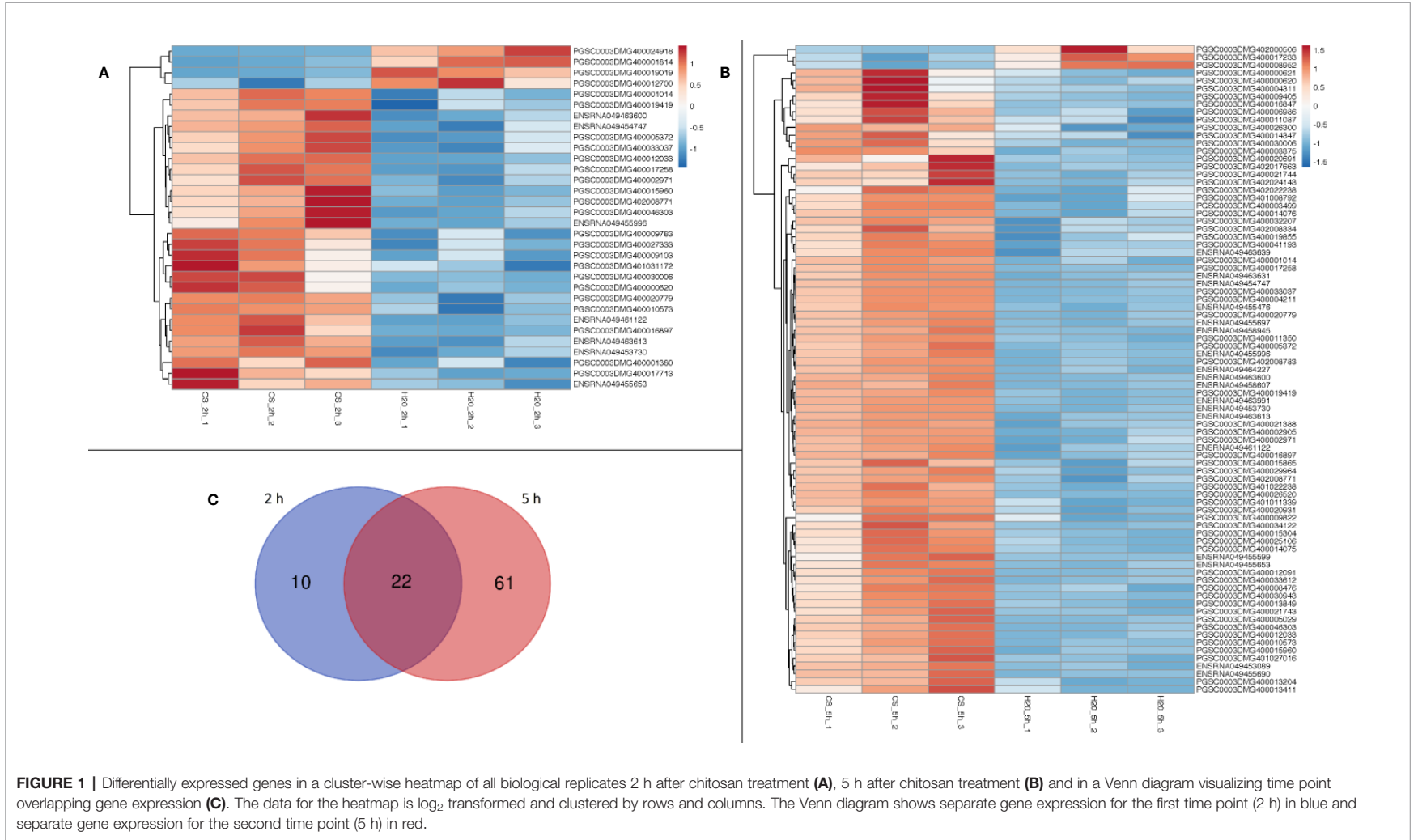
Functional annotation of downregulated genes showed that they include structural constituents of ribosomes and genes associated with peptide metabolic processes. Another downregulated DEG was identified as a CoA hydrolase and was observed enriched in the KEGG ribosome pathway. Furthermore, an ethylene-responsive transcription factor, identified enriched in a cellular defense response pathway and Alpha-DOX2, enriched in KEGG alpha-linolenic acid metabolism, were downregulated 5 h after chitosan treatment. However, none of the downregulated genes showed a similar expression pattern in both sample groups.

Chitosan Treatment Induces Few Genes Directly Involved in Disease Resistance

Although activation of plant defense is widely known as one of the main reactions of plants to chitosan, we observed expression of only few defense-related genes. Potentially defense-related genes that were upregulated 2 h after chitosan treatment coded for a leucine-rich repeat receptor like kinase (LRR-RLK) and a WRKY transcription factor (**Figure 2A**). In addition, genes coding for an extensin and a proline-rich cell wall protein, both involved in cell wall synthesis and alteration and hence with potential to participate in defense responses, were upregulated. Several defense- and stress-related genes were in addition upregulated 5 h after treatment, including genes coding for photoassimilate-responding proteins, as well as for proteins to withstand osmotic, salt, and drought stress (**Figure 2B**). This surprisingly low number of upregulated defense-associated genes may indicate that chitosan is inducing plant disease resistance in a rather indirect manner, by triggering alterations in gene expression predominantly targeting cellular functions not solely or directly involved in pathogen defense.

Chitosan Treatment Activates Mitochondrial Gene Expression

One major consequence of chitosan treatment was the activation of (nuclear) genes coding for mitochondrial proteins. For example, genes encoding for cytochrome c oxidase (mitochondrial complex IV) and ATP synthase subunits were upregulated already 2 h after chitosan treatment with further increasing expression at the later time point (**Figure 2C**). Especially 5 h after chitosan treatment several genes related to mitochondrial electron transport (and hence, cellular energy supply) were upregulated, e.g., further ATP synthase subunits and genes related to mitochondrial complexes I and II.
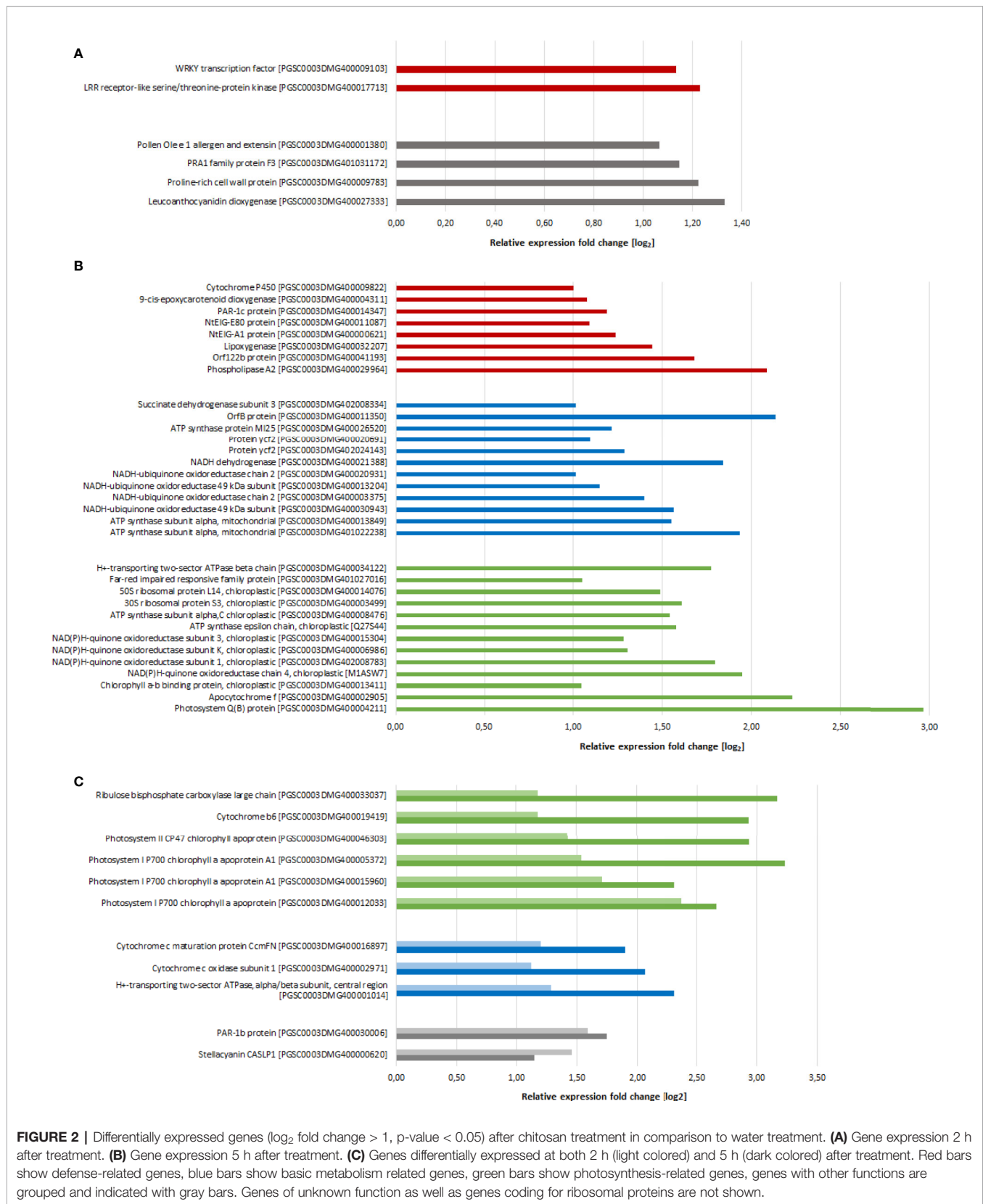
FIGURE 1 | Differentially expressed genes in a cluster-wise heatmap of all biological replicates 2 h after chitosan treatment **(A)**, 5 h after chitosan treatment **(B)** and in a Venn diagram visualizing time point overlapping gene expression **(C)**. The data for the heatmap is $\log_2$ transformed and clustered by rows and columns. The Venn diagram shows separate gene expression for the first time point (2 h) in blue and separate gene expression for the second time point (5 h) in red.

FIGURE 2 | Differentially expressed genes (log$_2$ fold change > 1, p-value < 0.05) after chitosan treatment in comparison to water treatment. **(A)** Gene expression 2 h after treatment. **(B)** Gene expression 5 h after treatment. **(C)** Genes differentially expressed at both 2 h (light colored) and 5 h (dark colored) after treatment. Red bars show defense-related genes, blue bars show basic metabolism related genes, green bars show photosynthesis-related genes, genes with other functions are grouped and indicated with gray bars. Genes of unknown function as well as genes coding for ribosomal proteins are not shown.

To illustrate the activation of electron transport in mitochondria, MapMan software with the "Mitochondrial_e-transport" pathway file was used (**Figure 3**). Corresponding genes were triggered both 2 and 5 h after chitosan treatment, indicated by upregulation of genes coding for subunits of complex I, cytochrome c protein, complex IV, and ATP synthase and further proven by a high enrichment of electron transfer activity on the molecular function (MF) level (**Figure 4**). As mentioned before, gene expression was stronger 5 h after chitosan treatment, and induction of genes coding for complex I was observed exclusively at this time point. Furthermore, ATP synthase gene expression was more strongly upregulated 5 h after chitosan treatment.

The upregulation of genes related to electron transport in mitochondria, especially with the increasing fold change over time, provides strong evidence for chitosan triggering mitochondrial cell activity as one of its main mechanism of action in the first hours after plant treatment.

Photosynthesis-Related Gene Induction Is the Main Response to Chitosan Treatment

While differential gene expression 2 h after chitosan treatment can be allocated to different biological functions, DEGs 5 h after treatment are mostly involved in photosynthesis and respiration (**Figures 2B, C**). For example, four different genes coding for subunits of the chloroplast NADH dehydrogenase-like (NDH) complex were upregulated. This was accompanied by upregulation of four genes coding for ATP synthase subunits. The highest upregulation of photosynthesis-related genes was displayed by genes coding for the PSII subunit D1 (*psbA*, 2.9-fold upregulation) and the cytochrome f subunit of the cytochrome b_6f complex (*petA*, 2.2-fold upregulation). Furthermore, from 11 genes that are upregulated at both time points (**Figure 2C**), six can be clearly allocated to the light phase of photosynthesis, including genes coding for PSI and PSII subunits. Furthermore, cytochrome b_6 subunit (*petB*) of the cytochrome b_6f complex was
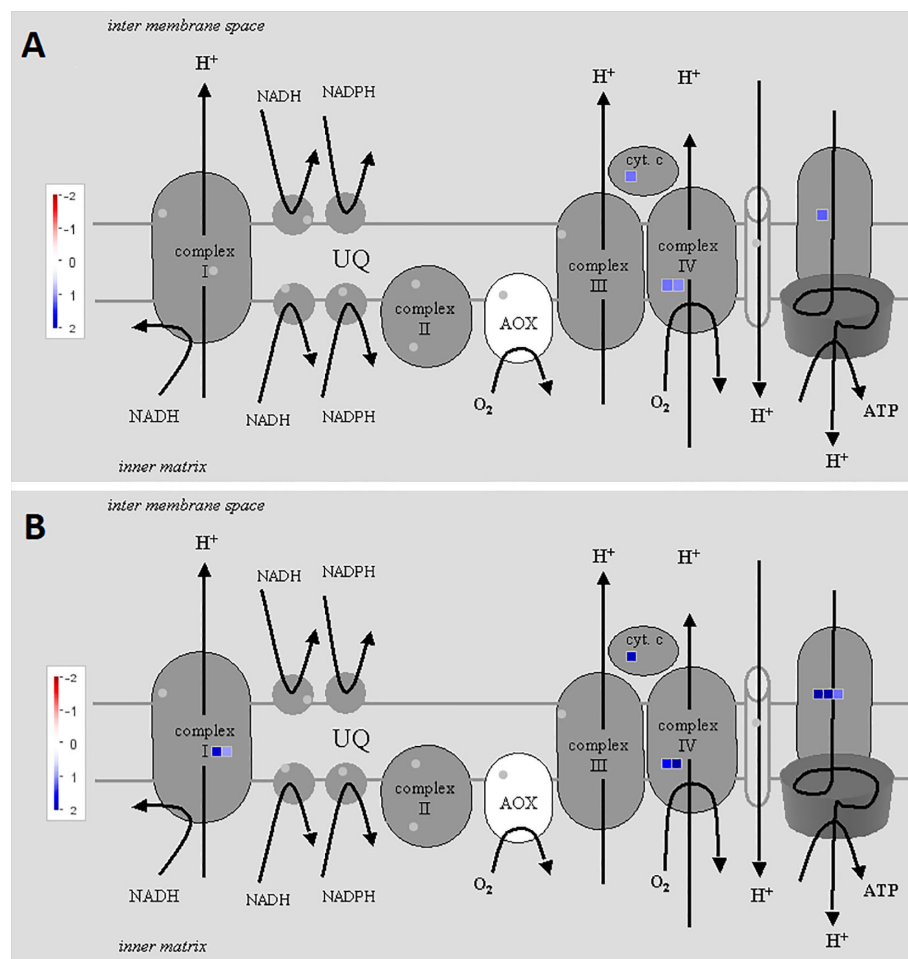

FIGURE 3 | Differentially expressed genes (DEGs) related to mitochondrial electron transport at time point 2 h **(A)** and 5 h **(B)**. The fold change was analyzed and allocated with MapMan software. Blue squares show the intensity of upregulation, where darker blue color indicates stronger upregulation. To visualize the pathway, Mitochondrial_e-transport 5.01 pathway was used. Stub_PGSC_DM_v3.4 was utilized for mapping as this mapping file represents the reference genome used for the sequencing. Both pathway and mapping were obtained from the MapMan website and are available through the Creative Common (CC) license. The mapping file did not cover all complex I and complex II related genes.
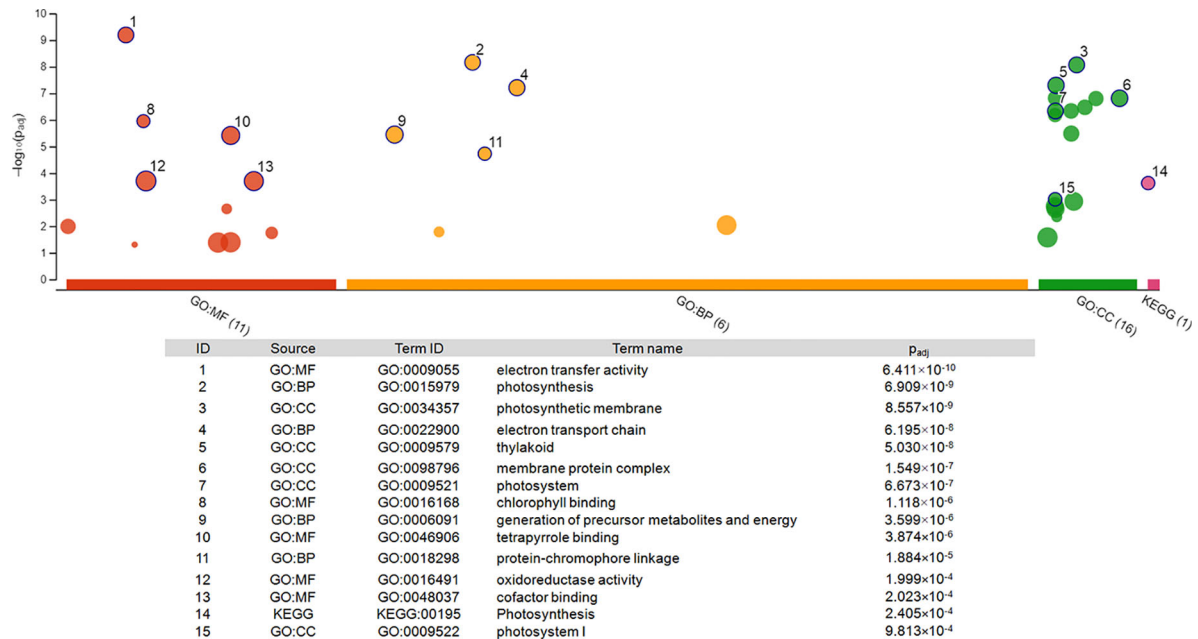
ID	Source	Term ID	Term name	P_{adj}
1	GO:MF	GO:0009055	electron transfer activity	6.411×10^{-10}
2	GO:BP	GO:0015979	photosynthesis	6.909×10^{-9}
3	GO:CC	GO:0034357	photosynthetic membrane	8.557×10^{-9}
4	GO:BP	GO:0022900	electron transport chain	6.195×10^{-8}
5	GO:CC	GO:0009579	thylakoid	5.030×10^{-8}
6	GO:CC	GO:0098796	membrane protein complex	1.549×10^{-7}
7	GO:CC	GO:0009521	photosystem	6.673×10^{-7}
8	GO:MF	GO:0016168	chlorophyll binding	1.118×10^{-6}
9	GO:BP	GO:0006091	generation of precursor metabolites and energy	3.599×10^{-6}
10	GO:MF	GO:0046906	tetrapyrrole binding	3.874×10^{-6}
11	GO:BP	GO:0018298	protein-chromophore linkage	1.884×10^{-5}
12	GO:MF	GO:0016491	oxidoreductase activity	1.999×10^{-4}
13	GO:MF	GO:0048037	cofactor binding	2.023×10^{-4}
14	KEGG	KEGG:00195	Photosynthesis	2.405×10^{-4}
15	GO:CC	GO:0009522	photosystem I	9.813×10^{-4}

FIGURE 4 | Pathway enrichment analysis of the 22 genes differentially expressed at both time points. The graph was generated *via* gProfiler service g:GOSt. X-axis represents grouped and color-coded functional GO terms (with numbers indicating the amount of significantly enriched terms in the corresponding source), y-axis shows the adjusted enrichment p-values in negative $\log_{10}$ scale. Dot size in the picture indicates the abundance of enriched genes in the functional groups. Numbers displayed on the dots are related to the details given in the table below the picture.

upregulated at both time points. These genes all showed higher upregulation after 5 h than after 2 h.

Functional enrichment of the 22 DEGs which showed upregulation at both 2 h and 5 h after chitosan treatment with iDEP demonstrated that upregulated DEGs were significantly enriched in six, mainly photosynthesis-related, pathways (**Figure 5A**). Interestingly, the most upregulated ($\log_2$ fold change ≥ 3) DEGs were identified enriched in the electron transport

pathways and photosynthesis, supporting our GO enrichment analysis (**Figure 3**), which showed that DEGs are related to photosynthesis pathways on the biological function (BF) and the cellular component (CC) levels.

To further analyze the interaction among the DEGs enriched in the MF, BF and CC pathways, a protein-protein-interaction (PPI) network was built *via* Search Tool for the Retrieval of Interacting Genes/Proteins (STRING, **Figure 5B**). This network
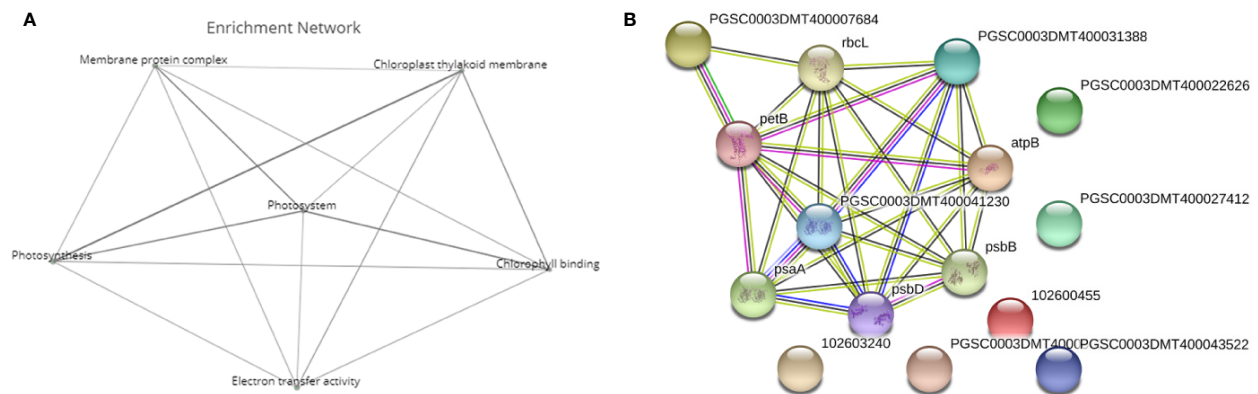

FIGURE 5 | Deeper analysis of pathway enrichment. **(A)** Enrichment network among the functional pathways. **(B)** Protein-protein interaction network generated *via* Search Tool for the Retrieval of Interacting Genes/Proteins (STRING) displaying the interaction among the genes in the enriched pathways. Four different evidence types were used to predict protein associations: black lines indicate coexpression evidence, green lines indicate neighborhood evidence, purple lines indicate experimental evidence and blue lines indicate cooccurrence evidence.
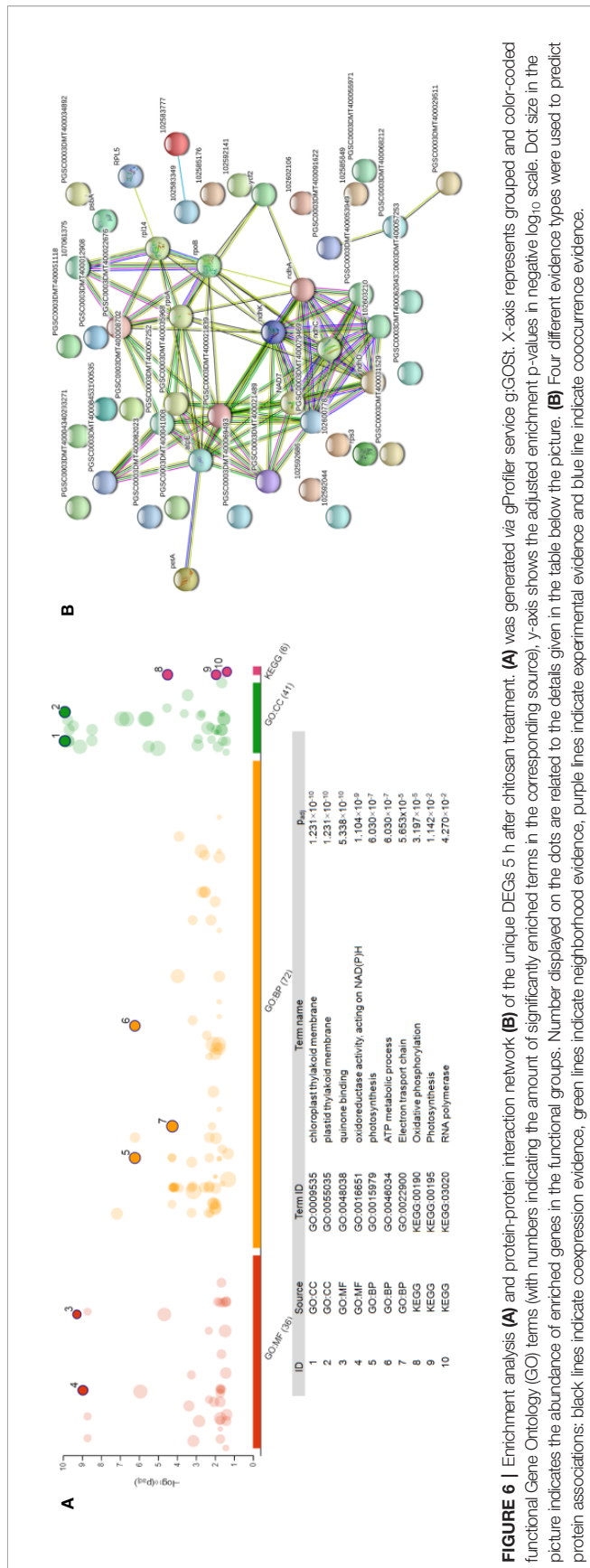
FIGURE 6 | Enrichment analysis **(A)** and protein-protein interaction network **(B)** of the unique DEGs 5 h after chitosan treatment. **(A)** was generated *via* gProfiler service g:GOSt. X-axis represents grouped and color-coded functional Gene Ontology (GO) terms (with numbers indicating the amount of significantly enriched terms in the corresponding source), y-axis shows the adjusted enrichment p-values in negative log₁₀ scale. Dot size in the picture indicates the abundance of enriched genes in the functional groups. Number displayed on the dots are related to the details given in the table below the picture. **(B)** Four different evidence types were used to predict protein associations: black lines indicate coexpression evidence, green lines indicate neighborhood evidence, purple lines indicate experimental evidence and blue line indicate cooccurrence evidence.

among the upregulated DEGs at both time points shed a light on the coexpression of the genes related to photosystems, electron transport and ATP synthesis and their connection in the enriched pathways. Upregulated and functionally annotated genes enriched in these pathways were psbA, psbB, and pdbD, coding for three essential subunits of photosystem II, petB, an important part of the cytochrome b₆f complex as well as rbcL, a gene coding for a RuBisCo subunit. **Figure 6** shows the enrichment analysis **(A)** and PPI **(B)** of DEGs upregulated 5 h after chitosan treatment and the relation among the genes linked to photosynthesis, ATP metabolism and oxidoreductase activity. Outstanding DEGs again included psbA and petA, similar to the PPI analysis 2 h after chitosan treatment, but also ndh and ATP synthase genes, likewise acting in photosynthesis. Cluster-wise analysis of DEGs at both time points emphasized the hypothesis of chitosan-dependent photosynthesis activation as all annotated pathways were linked to the light reaction (**Table 1**).

Gene categories containing genes that are upregulated 2 h after chitosan treatment (**Supplementary Table 4**) were mainly thylakoid components (GO:00095793), PSI (GO:0009522), and general photosynthesis processes (GO:0015979 and GO:0019684). The same genes were upregulated 5 h after chitosan treatment (**Supplementary Table 5**).

Figure 7 shows the upregulation of genes related to electron transport in the light reaction of photosynthesis in the chloroplast, visualized *via* MapMan (using the "ChloroPlast_CustomArray_CUSTOM_MAPPING" pathway file). Genes coding for subunits of PSII, cytochrome b₆f complex, and PSI were upregulated at both time points and upregulation was clearly stronger 5 h after chitosan treatment, including the upregulation of more genes for PSI subunits. In addition, D1, one of the two large subunits of PSII, was only upregulated 5 h after chitosan treatment. The largest difference between the two time points concerning chloroplast activity is the upregulation of five genes coding for ATP synthase subunits exclusively at 5 h after chitosan treatment (**Figure 7B**).

To further visualize the activation of photosynthesis-related genes, assignment of upregulated genes to their respective structure in the photosynthetic apparatus was also done *via* KEGG pathway map for the photosynthetic light reaction in potato (Ogata et al., 1999). The KEGG pathway map indicates the activation of genes coding for subunits of all four main light reaction components, namely PSII, cytochrome b₆f complex, PSI, and ATP synthase (**Supplementary Figure 4**), all of them encoded in the chloroplast (Rogalski et al., 2015).

TABLE 1 | Enriched pathways for each cluster.

Cluster	Adjusted p-value	Number of genes	Pathways
A	7.5e04	2	Photosystem I
	1.9e-03	2	Electron transport chain
	9.6e-03	2	Tetrapyrrole binding
B	6.8e-09	5	Photosynthesis
	6.8e-09	5	Electron transfer activity
	3.5e-08	5	Membrane protein complex

Cluster-wise enrichment analysis was conducted using R-based iDEP (integrated Differential Expression and Pathway analysis) online tool.
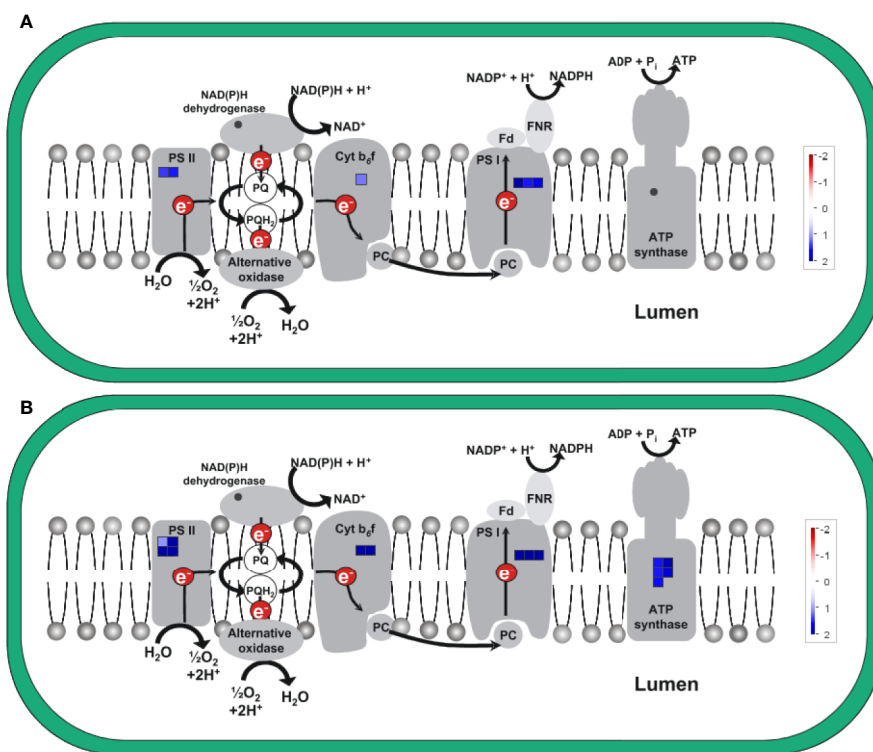
FIGURE 7 | Differentially expressed genes (DEGs) related to electron transport in the light reaction of photosynthesis in the chloroplast at time point 2 h **(A)** and 5 h **(B)**. The fold change was analyzed and allocated with MapMan software. Blue squares show the intensity of upregulation, where darker blue color indicates stronger upregulation. To visualize the pathway, ChloroPlast_CustomArray_CUSTOM_MAPPING 1 pathway was used. Stub_PGSC_DM_v3.4 was utilized for mapping as this mapping file represents the reference genome used for the sequencing. Both pathway and mapping were obtained from the MapMan website and are available through the Creative Common (CC) license. NDH complex is not covered by the pathway.

The significant upregulation of photosynthesis-related genes, mainly of the light reaction in chloroplasts, provides strong evidence that chitosan treatment is predominantly triggering increased electron transport in chloroplasts, eventually leading to higher concentrations of sugars and energy itself.

Validation of DEGs *via* qPCR

qPCR experiments were performed to validate the gene expression results obtained by RNA sequencing (**Figure 8**). The qPCR results were in agreement with the sequencing results, showing the similar relative expression increases from 2 h to 5 h after chitosan treatment. The Pearson correlation coefficient between RNAseq and qPCR data for the genes quantified 5 h after treatment was determined as 0.76, indicating a strong positive correlation.

Functional Analysis of Chitosan-Induced Reactions in Potato Leaves

The common theme during gene induction in chitosan-treated potato leaves appears to be a correlation with electron transport. As electron transfer from NAD(P)H to oxygen in a rapid and transient oxidative burst is a known central, orchestrating event in the elicitation of disease resistance reactions, we quantified the H_2O_2 production in potato leaf disks after chitosan treatment,

using the identical experimental setup as in the RNAseq experiment (**Figure 9**). We observed a typical oxidative burst reaction, with a fast onset, reaching a maximum at around 20 min and ending after around 90 min. Water treatment as a control did not result in an oxidative burst.

DISCUSSION

Chitosan treatments are long known to have the potential to protect plants, including potato, from disease, both owing to their direct antimicrobial activities and to the induction of the plant's own defense systems. As a consequence, we had expected to predominantly observe chitosan-induced upregulation of defense-related genes, e.g., coding for pathogenesis related proteins or enzymes involved in the biosynthesis of phytoalexins and other secondary metabolites. However, this is not what we found. Instead, we observed a rather specific upregulation of genes involved in electron transport chains of photosynthesis and, to a lesser extent, of respiration. While a positive influence of chitosan treatments on plant growth and development is also well established, most studies investigating the effect of chitosan on plant productivity focus on time points days and weeks after treatment [as, e.g., reviewed in (Malerba
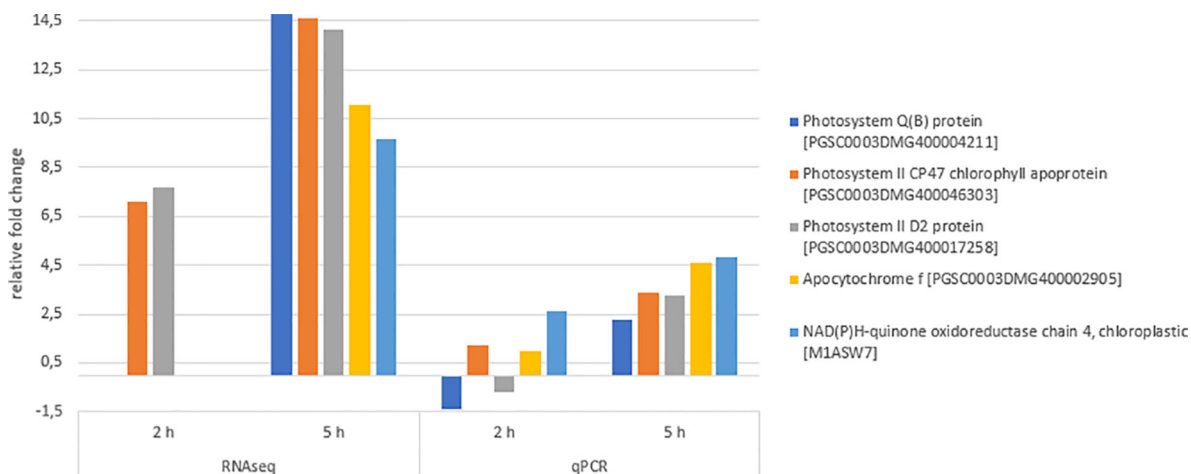
FIGURE 8 | Differentially expressed genes (DEGs) validation *via* quantitative PCR (qPCR). Expression fold change of qPCR values was calculated using the efficiency corrected calculation model described by (Pfaffl, 2001). Blue bars indicate fold change 2 h after treatment, orange bars indicate fold change 5 h after treatment. Given expression changes of qPCR values are relative to water treatment. The Pearson correlation coefficient of both RNAseq and qPCR values 5 h after chitosan treatment was determined as 0.76, indicating a strong positive correlation.

and Cerana, 2016)]. As in our study, we targeted the earliest plant responses to chitosan treatment, this influence on photosynthetic electron transport and energy metabolism was unexpected. We hence suggest that the here observed gene activation displays an initial spark for all further observations.

The strong upregulation of genes coding for proteins of every complex of the photosynthetic light reaction clearly points to an activation of photosynthesis and hence, energy production upon chitosan treatment. Concerning PSII as the first protein complex, we observed upregulation of both *psbA* and *psbD*, coding for D1

and D2, the two main subunits of the reactive center core of PSII (Marder et al., 1987). Enhanced gene expression of *psbA* and *psbD* was accompanied by upregulation of *psbB*, encoding the PSII chlorophyll-binding protein CP47, which forms the inner light-harvesting complex of PSII together with the *psbC*-product CP43 (Barber et al., 1997; Bricker and Frankel, 2002). As PSII is the strongest known natural oxidizing agent (Vrettos and Brudvig, 2002), it suffers from oxidative damage and therefore displays shorter lifetimes in comparison to other photosynthetic compounds, necessitating a particularly high turnover rate (Yao
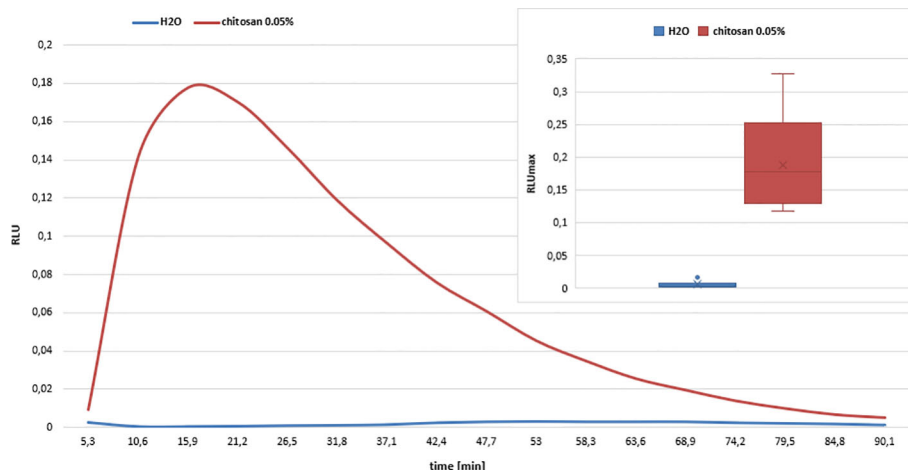

FIGURE 9 | Oxidative burst response of chitosan treated potato leaf disks. Chitosan (FA 0.2, DPw 515, Đ$_{DP}$ 2, 0.05%) elicits an oxidative burst reaction in potato leaf disks, as indicated by the rapid increase of relative light units (RLU) caused by H_2O_2 reaction with the luminol derivative L-012. Water-treatment of potato leaf disks did not result in any response. Reaction curves display mean values out of six technical replicates. Standard deviations are not shown to improve clarity. Box plots in the insert show the maximum RLU (RLUmax) values of chitosan- and water-treated potato leaves. The boxes contain 50% of all values with the median value given in a horizontal line and the mean vale given as a cross. The whiskers above and below the box represent data below the first or above the third quartile. Outliers are indicated as dots. The difference in response was significant according to one-way ANOVA analysis and *post hoc* Tukey test.

et al., 2012). Thus, increased photosynthetic activity will have to be accompanied by increased biosynthesis of the oxidatively damaged proteins. However, upregulation of PSII most likely not only serves protein replacement, but is also part of an overall increase in photosynthetic capacity. This conclusion is supported by the fact that apart from the photosystems, genes coding for proteins related to both the cytochrome b_6f complex and ATP synthase were upregulated. We observed significant upregulation of *petA* and *petB*, encoding the large subunits cytochrome f and cytochrome b_6 of the complex, which indicates an increased electron flux and, thus, and increased capacity for photosynthetic activity. It is known that cytochrome b_6f complex activity is closely linked to ATP synthase activity to ensure proton balance between stroma and lumen (Schöttler and Tóth, 2014). Accordingly, we observed upregulation of different subunits of the ATP synthase, namely genes encoding the α-subunits (*atpA*) as well as one gene each encoding a β-subunit (*atpB*) and a ε-subunit (*atpE*). All these upregulated genes encode proteins from the catalytic F_1 head of the chloroplast ATP synthase, where α and β-subunits form the rotating $α_3β_3$-subcomplex responsible for ATP formation (Hahn et al., 2018). coregulation of the cytochrome b_6f complex and the ATP synthase might provide evidence for a crosstalk between these complexes in potato, as generally assumed for higher plants (Schöttler and Tóth, 2014). In addition to linear electron transport, also cyclic electron transport appears to be enhanced, as indicated by upregulation of genes related to the type I NADPH dehydrogenase (NDH) complex responsible for cyclic electron transfer between PSI and the cytochrome b_6f complex (Burrows et al., 1998). It has been shown that cyclic electron transfer *via* the NDH complex plays an important role in both C_3 (Joet et al., 2002) and C_4 (Ishikawa et al., 2016) plants to satisfy increased ATP demands. Increased NDH complex activity has been linked to the mitigation of heat and light stress (Essemine et al., 2017), oxidative damage, and other stresses (Yamori and Shikanai, 2016). Overall, the changes in photosynthetic energy metabolism induced by chitosan treatment, thus, most likely contribute to increased disease resistance and abiotic stress tolerance.

Activation of photosynthesis in response to chitosan treatment fits well to other findings. As an example, chitosan treatment led to overexpression of photosynthesis-related genes in strawberry fruits (Landi et al., 2017), increasing the fruit yield by more than 40% (Akter Mukta et al., 2017). Similarly, chitosan treatment of rice plants resulted in increased photosynthesis rates and higher biomass (Phothi and Theerakarunwong, 2017). Both examples suggest that chitosan treatment not only triggers the expression of photosynthesis-related genes, but indeed leads to increased photosynthetic activity. Accordingly, proteomic analysis of chitosan-treated rice plants showed significant upregulation of proteins involved in photosynthesis, carbohydrate metabolism and cell redox homeostasis (Chamnanmanoontham et al., 2014). As this protein expression was observed 24 h after chitosan treatment, these findings are in agreement with our observations of an upregulation of the corresponding genes in the first hours after

chitosan treatment. Additionally, field trials with chitosan-treated potato plants resulted in up to 30% enhanced potato yields (Falcón-Rodríguez et al., 2017). Equally, foliar application of chitosan enhanced both growth and drought tolerance of potato plants (Muley et al., 2019). Based on our findings, this yield increase might be assigned to an activation of photosynthesis and resultant increased biomass production. Interestingly, potato virus Y infected potato plants show gene induction of photosynthesis-related processes including the light reaction within the first 12 h (Baebler et al., 2009) or 24 h (Stare et al., 2015) after inoculation. We therefore assume that chitosan treatment successfully mimics pathogen infection in potato, leading to a comparable response.

In our study, chitosan treatment induced genes coding for proteins involved in the electron transport chains of both the photosynthetic light reaction in the chloroplasts and the respiratory chain in the mitochondria. We observed upregulation of genes allocated to all protein complexes of the mitochondrial respiratory chain except for complex III. The respiratory electron transfer in plant mitochondria is not only important for energy supply *via* ATP synthesis, but can respond to different metabolic states of plant cells if altered due to environmental changes (Schertl and Braun, 2014). It is also known that not only the electron chain of the light reaction, but also the mitochondrial electron chain can react to light stress, e.g., supporting the chloroplasts to deal with excess NADPH (Yoshida et al., 2011). As several studies investigated the participation of mitochondria in producing ROS to regulate plant stress (Møller, 2001; Gleason et al., 2011; Huang S. et al., 2016), expression of mitochondrial respiratory chain-related genes might also be related to defense responses, as discussed below.

Increased activities of the photosynthetic and respiratory electron transfer chains will invariably lead to increased ROS production. In addition, both organelles are able to deliberately generate ROS as signal molecules (Foyer and Noctor, 2003) or antimicrobial agents (Choudhury et al., 2017), possibly even mediating and amplifying ROS signals deriving from the apoplast (Joo, 2005). While ROS concentrations are usually kept low by the action of detoxifying antioxidant systems, stress conditions can lead to retrograde ROS signaling (Navrot et al., 2007), e.g., between chloroplast and nucleus in the event of high light conditions (Galvez-Valdivieso and Mullineaux, 2010). In total, the formation of ROS in different cellular compartments in response to different conditions and their export into the cytosol establish extensive crosstalk of ROS in plant cells, integrating a broad range of cellular processes including gene expression, primary and secondary metabolism, and direct protection against diseases (Frederickson Matika and Loake, 2014). By regulating cellular redox homeostasis, ROS crosstalk ultimately provides information to the plant on the current energy status for growth and general development (Foyer and Noctor, 2009). Chitosan is well known to elicit an apoplastic oxidative burst in many plant species (Malerba and Cerana, 2016; Lopez-Moya et al., 2019). Recent *in vivo* quantification of intracellular H_2O_2 in *Arabidopsis* revealed that apoplastic ROS

can enter the cytosol and the mitochondrial matrix to modulate cell signals (Nietzel et al., 2018). Chitosan-triggered increased activities of organellar electron transport chains may well contribute to this complex ROS signaling.

It is furthermore well known that chitosan treatment can act as plant priming, enabling a faster and more efficient response to upcoming biotic or abiotic challenges (Frost et al., 2008; Mauch-Mani et al., 2017), and chitosan has recently been shown to induce priming in rice cells (Basa et al., 2020). Priming agents are thought to act on redox signaling, altering the overall oxidative environment of plant cells which eventually puts plants in an alarm state (González-Bosch, 2018). Our study suggests that chitosan-induced priming activity of chitosan may involve activation of redox-sensitive genes to support primary metabolism and defense preparation against prospective stress situation.

Upregulation of genes related to ROS formation in plant organelles in response to chitosan treatment may suggest prolonged ROS accumulation, not only for signaling and priming, but also directly serving disease resistance, as also suggested by chitosan-triggered defense-related gene expression. Particularly, we observed the early upregulation of a LRR-RLK and of one type of WRKY transcription factor. LRR-RLKs play central roles in signaling during pathogen perception (Afzal et al., 2008), while WRKY transcription factors constitute a major transcription factor family in plants, regulating a broad range of processes including biotic and abiotic stresses (Phukan et al., 2016). The here observed LRR-RLK was for instance also found to be upregulated in the wild potato Solanum commersonii upon Ralstonia solanacearum infection (Zuluaga et al., 2015), and LRR-RLKs are also known to be involved in ROS signaling (Eckardt, 2017). As no chitosan specific receptor has been described in plants so far, it is tempting to speculate that this LRR-RLK is involved in chitosan perception, possibly triggering a signal cascade involving mitogen-activated protein (MAP) kinases as described for chitin perception in rice and Arabidopsis plants (Kawasaki et al., 2017). Based on a classification by (Huang and Liu, 2013), the WRKY transcription factor found in this study is classified as StWRKY22, located on chromosome 3 and grouped into group III, the group that contains WRKY transcription factors influencing disease resistance (Wang et al., 2015; Huang Y. et al., 2016). Upregulation of both LRR-RLK and StWRKY22 clearly indicates that chitosan triggers defense responses in potato leaves within the first few hours after treatment. In addition, we observed upregulation of a lipoxygenase, an enzyme involved in the synthesis of many signaling compounds (Porta and Rocha-Sosa, 2002) and known to be induced during pathogen defense (Ocampo et al., 1986). The octadecanoid pathway in which lipoxygenase catalyzes the first step, results in the production of jasmonic acid (JA), an important signaling molecule mediating plant responses toward both biotic and abiotic stresses (Ruan et al., 2019). Chitosan -induced upregulation of lipoxygenase, thus, is in agreement with the long known JA accumulation in response to chitosan treatment (Doares et al., 2006; Kim et al., 2014).

Further evidence for a connection between upregulation of ROS-related genes and disease resistance and also for the already mentioned redox-sensitive priming activity of chitosan is provided by the observation of an oxidative burst response in potato leaf disks upon treatment with chitosan. Chitosan is well known to display eliciting activity in plants (Malerba and Cerana, 2016), possibly perceived via chitin receptors (Kaku et al., 2006; Gubaeva et al., 2018). Downstream signaling leading to the activation of plant immunity involves the generation of ROS, activation of phytohormone crosstalk, the production of pathogenesis-related proteins as well as other responses involved in warding off pathogens (Jones and Dangl, 2006). However, chitosans differ in their structural parameters such as their degree of polymerization and degree of acetylation, and both parameters strongly influence the biological activities of chitosans (Vander et al., 1998; Cord-Landwehr et al., 2020; Wattjes et al., 2020). Also, different plant species may react differently to the same chitosan (Santos et al., 2008). Therefore, it was important to show that the chitosan used for the transcriptomic study indeed induces a disease resistance response in the potato genotype used. As a central orchestrating event in the induction of resistance reactions and based on the observation of massive upregulation of genes encoding components of electron transport chains, we chose elicitation of the oxidative burst as a read-out in this functional verification experiment. The observed rapid and early ROS release via oxidative burst reactions in response to chitosan might explain the subsequent upregulation of ROS-related genes, as proteins involved in ROS signaling are vulnerable to damage via ROS scavenging or forwarding in signaling processes (Sharma et al., 2012). Hence, the observed upregulation of genes involved in ROS crosstalk might provide evidence for both a general armament of such structures and a replacement of already exhausted structures through the observed, preceding oxidative burst reactions, providing new insights for a functional connection between nucleus-dependent and nucleus-independent signaling pathways of chitosan triggered ROS reactions (Schmitt et al., 2014). Clearly, the here described transcriptomic approach should be complemented in future by a metabolomic study in order to gain a more comprehensive understanding of chitosan-triggered immunity. In addition, observation of both upregulation of ROS-related genes, eventually supporting photosynthesis, and the oxidative burst itself provides evidence for a positive feedback of primary metabolism and defense, as sugar concentrations are known to regulate ROS generation and removal (Couée et al., 2006; Keunen et al., 2013). Furthermore, ROS are known to influence plant growth as they tend to accumulate in meristems (Huang et al., 2019).In this study, surprisingly few genes were significantly overexpressed in comparison to transcriptomic approaches of chitosan-treated strawberry (Landi et al., 2017) and avocado (Xoca-Orozco et al., 2017) fruits. While the treatment in this study was based on a well-characterized, pure chitosan that has been optimized for plant disease protection, a standard commercial chitosan sourced from

Sigma-Aldrich was used for the avocado treatment, and a chitosan-based commercial product from ChiPro GmbH for strawberry treatment. Also, to avoid nonspecific stress reactions, we used our chitosan at a very low concentration (0.05%) which we know to give optimal plant protection, while much higher concentrations were used in the other studies (1.5% in avocado, 1% in strawberry). Hence, we believe that one reason for the comparably high number of differential gene expression in the other studies might be the usage of less characterized or less pure chitosans at much higher concentrations, leading to nonspecific effects.

In summary, our study demonstrates that chitosan perception leads to an activation of primary metabolism and thus, indirectly, plant defense. The strongly dominating focus on electron chains in chloroplasts and mitochondria indicates increased energy production and intracellular crosstalk, ultimately resulting in a more productive metabolic state. These responses concomitantly contribute to the often described increased disease resistance and abiotic stress tolerance as well as promotion of plant growth and development upon chitosan treatment, leading to higher productivity of crop plants upon chitosan treatment.

DATA AVAILABILITY STATEMENT

The datasets presented in this study can be found in online repositories. The names of the repository/repositories and accession number(s) can be found below: https://www.ebi.ac.uk/ena/browser, PRJEB36930.

REFERENCES

Afzal, A. J., Wood, A. J., and Lightfoot, D. A. (2008). Plant Receptor-Like Serine Threonine Kinases: Roles in Signaling and Plant Defense. *Mol. Plant-Microbe Interact.* 21 (5), 507–517. doi: 10.1094/mpmi-21-5-0507

Akimoto-Tomiyama, C., Sakata, K., Yazaki, J., Nakamura, K., Fujii, F., Shimbo, K., et al. (2003). Rice Gene Expression in Response to N-Acetylchitooligosaccharide Elicitor: Comprehensive Analysis by DNA Microarray with Randomly Selected ESTs. *Plant Mol. Biol.* 52 (3), 537–551. doi: 10.1023/A:1024890601888

Akter Mukta, J., Rahman, M., Sabir, A. A., Gupta, D. R., Surovy, M. Z., Rahman, M., et al. (2017). Chitosan and Plant Probiotics Application Enhance Growth and Yield of Strawberry. *Biocatalysis Agric. Biotechnol.* 11, 9–18. doi: 10.1016/j.bcab.2017.05.005

Albert, M., and Fürst, U. (2017). Quantitative Detection of Oxidative Burst upon Activation of Plant Receptor Kinases. *Methods Mol. Biol.* 1621, 69–76. doi: 10.1007/978-1-4939-7063-6_7

Baebler, Š, Krečič-Stres, H., Rotter, A., Kogovšek, P., Cankar, K., Kok, E. J., et al. (2009). PVYNTN Elicits a Diverse Gene Expression Response in Different Potato Genotypes in the First 12 h after Inoculation. *Mol. Plant Pathol.* 10 (2), 263–275. doi: 10.1111/j.1364-3703.2008.00530.x

Barber, J., Nield, J., Morris, E. P., Zheleva, D., and Hankamer, B. (1997). The Structure, Function and Dynamics of Photosystem Two. *Physiologia Plantarum* 100 (4), 817–827. doi: 10.1034/j.1399-3054.1997.1000408.x

Basa, S., Nampally, M., Honorato, T., Das, S. N., Podile, A. R., El Gueddari, N. E., et al. (2020). The Pattern of Acetylation Defines the Priming Activity of Chitosan Tetramers. *J. Am. Chem. Soc.* doi: 10.1021/jacs.9b11466

Bautista-Baños, S., Hernández-Lauzardo, A. N., Velázquez-Del Valle, M. G., Hernández-López, M., Ait Barka, E., Bosquez-Molina, E., et al. (2006). Chitosan as a Potential Natural Compound to Control Pre and Postharvest

Diseases of Horticultural Commodities. *Crop Prot.* 25 (2), 108–118. doi: 10.1016/j.cropro.2005.03.010

Bredow, M., Sementchoukova, I., Siegel, K., and Monaghan, J. (2019). Pattern-Triggered Oxidative Burst and Seedling Growth Inhibition Assays in Arabidopsis Thaliana. *J. Visualized Experiments.* 147. doi: 10.3791/59437

Bricker, T. M., and Frankel, L. K. (2002). The Structure and Function of CP47 and CP43 in Photosystem II. *Photosynthesis Res.* 72 (2), 131–146. doi: 10.1023/A:1016128715865

Burlingame, B., Mouillé, B., and Charrondière, R. (2009). Nutrients, Bioactive Non-Nutrients and Anti-Nutrients in Potatoes. *J. Food Composition Anal.* 22 (6), 494–502. doi: 10.1016/j.jfca.2009.09.001

Burrows, P. A., Sazanov, L. A., Svab, Z., Maliga, P., and Nixon, P. J. (1998). Identification of a Functional Respiratory Complex in Chloroplasts through Analysis of Tobacco Mutants Containing Disrupted Plastid Ndh Genes. *EMBO J.* 17 (4), 868–876. doi: 10.1093/emboj/17.4.868

Chamnanmanoontham, N., Pongprayoon, W., Pichayangkura, R., Roytrakul, S., and Chadchawan, S. (2014). Chitosan Enhances Rice Seedling Growth via Gene Expression Network between Nucleus and Chloroplast. *Plant Growth Regul.* 75, 101–114. doi: 10.1007/s10725-014-9935-7

Chang, T., and Kim, B. S. (2012). Application of Chitosan Preparations for Eco-Friendly Control of Potato Late Blight. *Res. Plant Dis.* 18(4), 338–348. doi: 10.5423/rpd.2012.18.4.338

Chirkov, S. N., Il'ina, A. V., Surgucheva, N. A., Letunova, E. V., Varitsev, Y., Tatarinova, N., et al. (2001). Effect of Chitosan on Systemic Viral Infection and Some Defense Responses in Potato Plants. *Russian J. Plant Physiol.* 48, 774–779. doi: 10.1023/A:1012508625017

Choudhury, F. K., Rivero, R. M., Blumwald, E., and Mittler, R. (2017). Reactive Oxygen Species, Abiotic Stress and Stress Combination. *Plant J.* 90 (5), 856–867. doi: 10.1111/tpj.13299

AUTHOR CONTRIBUTIONS

FUNDING

ACKNOWLEDGMENTS

SUPPLEMENTARY MATERIAL

The Supplementary Material for this article can be found online at: https://www.frontiersin.org/articles/10.3389/fpls.2020.01193/full#supplementary-material

Cord-Landwehr, S., Richter, C., Wattjes, J., Sreekumar, S., Singh, R., Basa, S., et al. (2020). Patterns Matter Part 2: Chitosan Oligomers with Defined Patterns of Acetylation. *Reactive Funct. Polymers*. 151. doi: 10.1016/j.reactfunctpolym.2020.104577

Couée, I., Sulmon, C, Gouesbet, G., and Amrani, A. E. (2006). Involvement of Soluble Sugars in Reactive Oxygen Species Balance and Responses to Oxidative Stress in Plants. *J. Exp. Bot.* 57(3), 449–459 doi: 10.1093/jxb/erj027

Doares, S. H., Syrovets, T., Weiler, E. W., and Ryan, C. A. (2006). Oligogalacturonides and Chitosan Activate Plant Defensive Genes through the Octadecanoid Pathway. *Proc. Natl. Acad. Sci.* 92 (10), 4095–4098. doi: 10.1073/pnas.92.10.4095

Dobin, A., Davis, C. A., Schlesinger, F., Drenkow, J., Zaleski, C., Jha, S., et al. (2013). STAR: Ultrafast Universal RNA-Seq Aligner. *Bioinformatics* 29 (1), 15–21. doi: 10.1093/bioinformatics/bts635

Eckardt, N. A. (2017). The Plant Cell Reviews Plant Immunity: Receptor-Like Kinases, ROS-RLK Crosstalk, Quantitative Resistance, and the Growth/Defense Trade-Off. *Plant Cell* 29 (4), 601–602. doi: 10.1105/tpc.17.00289

Essemine, J., Xiao, Y., Qu, M., Mi, H., and Zhu, X.-G. (2017). Cyclic Electron Flow May Provide Some Protection against PSII Photoinhibition in Rice (Oryza Sativa L.) Leaves under Heat Stress. *J. Plant Physiol.* 211, 138–146. doi: 10.1016/j.jplph.2017.01.007

Falcón-Rodríguez, A. B., Costales, D., Gónzalez-Peña, D., Morales, D., Mederos, Y., Jerez, E., et al. (2017). Chitosans of Different Molecular Weight Enhance Potato (Solanum Tuberosum L.) Yield in a Field Trial. *Spanish J. Agric. Res.* 15 (1). doi: 10.5424/sjar/2017151-9288

Foyer, C. H., and Noctor, G. (2003). Redox Sensing and Signalling Associated with Reactive Oxygen in Chloroplasts, Peroxisomes and Mitochondria. *Physiologia Plantarum*. 119 (3), 355–364 doi: 10.1034/j.1399-3054.2003.00223.x

Foyer, C. H., and Noctor, G. (2009). Redox Regulation in Photosynthetic Organisms: Signaling, Acclimation, and Practical Implications. *Antioxidants Redox Signaling* 11 (4), 861–905. doi: 10.1089/ars.2008.2177

Frederickson Matika, D. E., and Loake, G. J. (2014). Redox Regulation in Plant Immune Function. *Antioxidants Redox Signaling.* 21 (9), 1373–1388. doi: 10.1089/ars.2013.5679

Frenkel, E. (2009). Gauge Theory and Langlands Duality. *Asterisque* 332, 369–403.

Frost, C. J., Mescher, M. C., Carlson, J. E., and De Moraes, C. M. (2008). Plant Defense Priming against Herbivores: Getting Ready for a Different Battle. *Plant Physiol.* 146 (3), 818–824. doi: 10.1104/pp.107.113027

Galvez-Valdivieso, G., and Mullineaux, P. M. (2010). The Role of Reactive Oxygen Species in Signalling from Chloroplasts to the Nucleus. *Physiologia Plantarum.* 138 (4), 430–509. doi: 10.1111/j.1399-3054.2009.01331.x

Ge, S. X., Son, E. W., and Yao, R. (2018). IDEP: An Integrated Web Application for Differential Expression and Pathway Analysis of RNA-Seq Data. *BMC Bioinf.* 19 (1), 534. doi: 10.1186/s12859-018-2486-6

Gleason, C., Huang, S., Thatcher, L. F., Foley, R. C., Anderson, C. R., Carroll, A. J., et al. (2011). Mitochondrial Complex II Has a Key Role in Mitochondrial-Derived Reactive Oxygen Species Influence on Plant Stress Gene Regulation and Defense. *Proc. Natl. Acad. Sci.* 108 (26), 10768–10773. doi: 10.1073/pnas.1016060108

Gong, L., Zhang, H., Gan, X., Zhang, L., Chen, Y., Nie, F., et al. (2015). Transcriptome Profiling of the Potato (Solanum Tuberosum L.) Plant under Drought Stress and Water-Stimulus Conditions. Edited by Binying Fu. *PLoS One* 10 (5), e0128041. doi: 10.1371/journal.pone.0128041

González-Bosch, C. (2018). Priming Plant Resistance by Activation of Redox-Sensitive Genes. *Free Radical Biol. Med*. 122, 171–180. doi: 10.1016/j.freeradbiomed.2017.12.028

Goyer, A., Hamlin, L., Crosslin, J. M., Buchanan, A., and Chang, J. H. (2015). RNA-Seq Analysis of Resistant and Susceptible Potato Varieties during the Early Stages of Potato Virus Y Infection. *BMC Genomics* 16 (1), 472. doi: 10.1186/s12864-015-1666-2

Gubaeva, E., Gubaev, A., Melcher, R. L.J., Cord-Landwehr, S., Singh, R., El Gueddari, N. E., et al. (2018). Slipped Sandwich' Model for Chitin and Chitosan Perception in Arabidopsis. *Mol. Plant-Microbe Interact.* 31 (11), 1145–1153. doi: 10.1094/MPMI-04-18-0098-R

Gueddari, N. E. E., and Moerschbacher, B. M. (2004). A Bioactivity Matrix for Chitosans as Elicitors of Disease Resistance Reactions in Wheat. *Adv. Chitin Sci. Volume VII* 7, 56–59.

Hadrami, A. E., Adam, L. R., Hadrami, I. E., and Daayf, F. (2010). Chitosan in Plant Protection. *Marine Drugs* 8 (4), 968–987. doi: 10.3390/md8040968

Hahn, A., Vonck, J., Mills, D. J., Meier, T., and Kühlbrandt, W. (2018). Structure, Mechanism, and Regulation of the Chloroplast ATP Synthase. *Science* 360 (6389), eaat4318. doi: 10.1126/science.aat4318

Hirai, A., Odani, H., and Nakajima, A. (1991). Determination of Degree of Deacetylation of Chitosan by 1H NMR Spectroscopy. *Polymer Bull.* 26, 87–94. doi: 10.1007/BF00299352

Hochberg, B. (1995). Controlling the False Discovery Rate: A Practical and Powerful Approach to Multiple Testing. *J. R. Stat. Soc.* 57 (1), 289–300. doi: 10.2307/2346101

Huang, S., and Liu, Y. (2013). Genome-Wide Analysis of WRKY Transcription Factors in Solanum Tuberosum. *Chin. J. Appplied Environ. Biol.* 19 (2), 205–214. doi: 10.3724/SP.J.1145.2013.00205

Huang, S., Aken, O. V., Schwarzländer, M., Belt, K., and Millar, A.H. (2016). The Roles of Mitochondrial Reactive Oxygen Species in Cellular Signaling and Stress Response in Plants. *Plant Physiol.* 171 (3), 1551–1559. doi: 10.1104/pp.16.00166

Huang, Y., Li, M. Y., Wu, P., Xu, Z. S., Que, F., Wang, F., et al. (2016). Members of WRKY Group III Transcription Factors Are Important in TYLCV Defense Signaling Pathway in Tomato (Solanum Lycopersicum). *BMC Genomics* 17 (1), 1551–1559. doi: 10.1186/s12864-016-3123-2

Huang, H., Ullah, F., Zhou, D. X., Yi, M., and Zhao, Y. (2019). Mechanisms of ROS Regulation of Plant Development and Stress Responses. *Front. Plant Sci.* 10, 800. doi: 10.3389/fpls.2019.00800

Ippólito, S. D., Mendieta, J. R., Terrile, M. C., Tonón, C. V., Mansilla, A. Y., Colman, S., et al. (2017). "Chitosan as Source for Pesticide Formulations," in *Biological Activities and Application of Marine Polysaccharides*, Chapter 1, 3–15. doi: 10.5772/65588

Iriti, M., and Faoro, F. (2009). Chitosan as a MAMP, Searching for a PRR. *Plant Signaling Behav.* 4 (1), 66–68. doi: 10.4161/psb.4.1.7408

Ishikawa, N., Takabayashi, A., Noguchi, K., Tazoe, Y., Yamamoto, H., von Caemmerer, S., et al. (2016). NDH-Mediated Cyclic Electron Flow Around Photosystem I Is Crucial for C 4 Photosynthesis. *Plant Cell Physiol.* 57 (10), 2020–2028. doi: 10.1093/pcp/pcw127

Jia, X., Meng, Q., Zeng, H., Wang, W., and Yin, H. (2016). Chitosan Oligosaccharide Induces Resistance to Tobacco Mosaic Virus in Arabidopsis via the Salicylic Acid-Mediated Signalling Pathway. *Sci. Rep.* 6 (1):26144. doi: 10.1038/srep26144

Joet, T., Cournac, L., Peltier, G., and Havaux, M. (2002). Cyclic Electron Flow around Photosystem I in C3 Plants. In Vivo Control by the Redox State of Chloroplasts and Involvement of the NADH-Dehydrogenase Complex. *Plant Physiol.* 128 (2), 760–769. doi: 10.1104/pp.010775

Jones, J. D.G., and Dangl, J. L. (2006). The Plant Immune System. *Nature* 444 (7117), 323–329. doi: 10.1038/nature05286

Joo, J. H. (2005). Different Signaling and Cell Death Roles of Heterotrimeric G Protein and Subunits in the Arabidopsis Oxidative Stress Response to Ozone. *Plant Cell Online* 17 (3), 957–970. doi: 10.1105/tpc.104.029603

Kaku, H., Nishizawa, Y., Ishii-Minami, N., Akimoto-Tomiyama, C., Dohmae, N., Takio, K., et al. (2006). Plant Cells Recognize Chitin Fragments for Defense Signaling through a Plasma Membrane Receptor. *Proc. Natl. Acad. Sci.* 103 (29), 11086–11091. doi: 10.1073/pnas.0508882103

Kanehisa, M., Furumichi, M., Tanabe, M., Sato, Y., and Morishima, K. (2017). KEGG: New Perspectives on Genomes, Pathways, Diseases and Drugs. *Nucleic Acids Res.* 45, D353–D361. doi: 10.1093/nar/gkw1092

Kanehisa, M., Sato, Y., Furumichi, M., and Tanabe, M. (2019). New Approach for Understanding Genome Variations in KEGG. *Nucleic Acids Res.* 47 (D1), D590–D595. doi: 10.1093/nar/gky962

Katiyar, D., Hemantaranjan, A., Singh, B., and Bhanu, A.N. (2014). A Future Perspective in Crop Protection: Chitosan and Its Oligosaccharides. *Adv. Plants Agric. Res.* 1 (1), 4–11. doi: 10.15406/apar.2014.01.00006

Kawasaki, T., Yamada, K., Yoshimura, S., and Yamaguchi, K. (2017). Chitin Receptor-Mediated Activation of MAP Kinases and ROS Production in Rice and Arabidopsis. *Plant Signaling Behav.* 12 (9), e1361076. doi: 10.1080/15592324.2017.1361076

Keunen, E., Peshev, D., Vangronsveld, J., Van Den Ende, W., and Cuypers, A. (2013). Plant Sugars Are Crucial Players in the Oxidative Challenge during

Abiotic Stress: Extending the Traditional Concept. *Plant Cell Environ*. 36 (7), 1242–1255. doi: 10.1111/pce.12061

Kim, Y., Tsuda, K., Igarashi, D., Hillmer, R. A., Sakakibara, H., Myers, C. L., et al. (2014). Signaling Mechanisms Underlying the Robustness and Tunability of the Plant Immune Network. *Cell Host Microbe*. 15 (1), 84–94. doi: 10.1016/j.chom.2013.12.002.Signaling

Kolde, R. (2019). *Pheatmap: Pretty Heatmaps. R Package Version 1.0.10. 2019*. https://cran.r-project.org/package=pheatmap.

Krueger, F. (2018). *Trim Galore! 2018*. http://www.bioinformatics.babraham.ac.uk/projects/trim_galore/.

Kulikov, S. N., Chirkov, S. N., Il'ina, A. V., Lopatin, S. A., Varlamov, V. P., Il'ina, A. V., et al. (2006). Effect of the Molecular Weight of Chitosan on Its Antiviral Activity in Plants. *Appl. Biochem. Microbiol*. 42 (2), 200–203. doi: 10.1134/s0003683806020165

Landi, L., Angelini, R. M. D. M., Pollastro, S., Feliziani, E., Faretra, F., and Romanazzi, G. (2017). Global Transcriptome Analysis and Identification of Differentially Expressed Genes in Strawberry after Preharvest Application of Benzothiadiazole and Chitosan. *Front. Plant Sci*. 8:235. doi: 10.3389/fpls.2017.00235

Lavertu, M., Xia, Z., Serreqi, A. N., Berrada, M., Rodrigues, A., Wang, D., et al. (2003). A Validated 1H NMR Method for the Determination of the Degree of Deacetylation of Chitosan. *J. Pharm. Biomed. Anal*. 32 (6), 1149–1158. doi: 10.1016/S0731-7085(03)00155-9

Lopez-Moya, F., Suarez-Fernandez, M., and Lopez-Llorca, L. V. (2019). Molecular Mechanisms of Chitosan Interactions with Fungi and Plants. *Int. J. Mol. Sci*. 20 (2), 332. doi: 10.3390/ijms20020332

Love, M.II, Huber, W., and Anders, S. (2014). Moderated Estimation of Fold Change and Dispersion for RNA-Seq Data with DESeq2. *Genome Biol*. 15 (12):550. doi: 10.1186/s13059-014-0550-8

Malerba, M., and Cerana, R. (2016). Chitosan Effects on Plant Systems. *Int. J. Mol. Sci*. 17 (7):996. doi: 10.3390/ijms17070996

Marder, J. B., Chapman, D. J., Telfer, A., Nixon, P. J., and Barber, J. (1987). Identification of PsbA and PsbD Gene Products, D1 and D2, as Reaction Centre Proteins of Photosystem 2. *Plant Mol. Biol*. 9 (4), 325–333. doi: 10.1007/BF00014907

Massa, A. N., Childs, K. L., Lin, H., Bryan, G. J., Giuliano, G., and Buell, C.R. (2011). The Transcriptome of the Reference Potato Genome Solanum Tuberosum Group Phureja Clone DM1-3 516R44. Edited by Jianwei Zhang. *PLoS One* 6 (10), e26801. doi: 10.1371/journal.pone.0026801

Massa, A. N., Childs, K. L., and Buell, C.R. (2013). Abiotic and Biotic Stress Responses in Group Phureja DM1-3 516 R44 as Measured through Whole Transcriptome Sequencing. *Plant Genome* 6 (3). doi: 10.3835/plantgenome2013.05.0014

Mauch-Mani, B., Baccelli, I., Luna, E., and Flors, V. (2017). Defense Priming: An Adaptive Part of Induced Resistance. *Annu. Rev. Plant Biol*. 68, 485–512. doi: 10.1146/annurev-arplant-042916-041132

Meurk, C., Broom, A., Adams, J., and Sibbritt, D. (2013). Rurality, Mobility, Identity: Women's Use of Complementary and Alternative Medicine in Rural Australia. *Health Place* 20, 75–80. doi: 10.1016/j.healthplace.2012.12.005

Miller, R. N. G., Alves, G. S. C., and Sluys, M. A. V. (2017). Plant Immunity: Unravelling the Complexity of Plant Responses to Biotic Stresses. *Ann. Bot*. 119 (5), 681–687 .doi: 10.1093/aob/mcw284

Møller, I. M. (2001). Plant Mitochondria and Oxidative Stress: Electron Transport, NADPH Turnover, and Metabolism of Reactive Oxygen Species. *Annu. Rev. Plant Physiol. Plant Mol. Biol*. 52 (1), 561–591. doi: 10.1146/annurev.arplant.52.1.561

Muley, A. B., Shingote, P. R., Patil, A. P., Dalvi, S. G., and Suprasanna, P. (2019). Gamma Radiation Degradation of Chitosan for Application in Growth Promotion and Induction of Stress Tolerance in Potato (Solanum Tuberosum L.). *Carbohydr. Polymers* 210, 289–301. doi: 10.1016/j.carbpol.2019.01.056

Muthoni, J., Kabira, J., Shimelis, H., and Melis, R. (2015). Tetrasomic Inheritance in Cultivated Potato and Implications in Conventional Breeding. *Aust. J. Crop Sci*. 9 (3), 185–190. doi: 10.1016/j.ymben.2006.08.006

Navrot, N., Rouhier, N., Gelhaye, E., and Jacquot, J. P. (2007). Reactive Oxygen Species Generation and Antioxidant Systems in Plant Mitochondria, *Physiologia Plantarum* 129 (1), 185–195. doi: 10.1111/j.1399-3054.2006.00777.x

Nicot, N., Hausman, J. F., Hoffmann, L., and Evers, D. (2005). Housekeeping Gene Selection for Real-Time RT-PCR Normalization in Potato during Biotic and Abiotic Stress. *J. Exp. Bot*. 56 (421), 2907–2914. doi: 10.1093/jxb/eri285

Nietzel, T., Elsässer, M., Ruberti, C., Steinbeck, J., Ugalde, J. M., Fuchs, P., et al. (2018). The Fluorescent Protein Sensor RoGFP2-Orp1 Monitors in Vivo H2O2 and Thiol Redox Integration and Elucidates Intracellular H2O2 Dynamics during Elicitor-induced Oxidative Burst in Arabidopsis. *New Phytol*. 221 (3), nph.15550. doi: 10.1111/nph.15550

Nishinaka, Y., Aramaki, Y., Yoshida, H., Masuya, H., Sugawara, T., and Ichimori, Y. (1993). A New Sensitive Chemiluminescence Probe, L-012, for Measuring the Production of Superoxide Anion by Cells. *Biochem. Biophys. Res. Commun*. 193 (2), 554–559. doi: 10.1006/bbrc.1993.1659

Ocampo, C. A., Moerschbacher, B., and Grambow, H. J. (1986). Increased Lipoxygenase Activity Is Involved in the Hypersensitive Response of Wheat Leaf Cells Infected with Avirulent Rust Fungi or Treated with Fungal Elicitor. *Z. Fur Naturforschung - Section C J. Biosci*. 41c, 559–563 .doi: 10.1515/znc-1986-5-612

Ogata, H., Goto, S., Sato, K., Fujibuchi, W., Bono, H., and Kanehisa, M. (1999). KEGG: Kyoto Encyclopedia of Genes and Genomes. *Nucleic Acids Res*. 27 (1), 29–34. doi: 10.1093/nar/27.1.29

Omura, Y., Shigemoto, M., Akiyama, T., Saimoto, H., Shigemasa, Y., Nakamura, I., et al. (2003). Antimicrobial Activity of Chitosan with Different Degrees of Acetylation and Molecular Weights. *Biocontrol Sci*. 8 (1), 25–30. doi: 10.4265/bio.8.25

O'Herlihy, E. A., Duffy, E. M., and Cassells, A. C. (2003). The Effects of Arbuscular Mycorrhizal Fungi and Chitosan Sprays on Yield and Late Blight Resistance in Potato Crops from Microplants. *Folia Geobotanica* 38, 201–207. doi: 10.1007/BF02803152

Pfaffl, M. W. (2001). A New Mathematical Model for Relative Quantification in Real-Time RT-PCR. *Nucleic Acids Res*. 29 (9), e45 doi: 10.1093/nar/29.9.e45

Pfaffl, M. W. (2002). Relative Expression Software Tool (REST(C)) for Group-Wise Comparison and Statistical Analysis of Relative Expression Results in Real-Time PCR. *Nucleic Acids Res*. 30 (9), 36e –3 36. doi: 10.1093/nar/30.9.e36

Phothi, R., and Theerakarunwong, C. D. (2017). Effect of Chitosan on Physiology, Photosynthesis and Biomass of Rice (Oryza Sativa L.) under Elevated Ozone. *Aust. J. Crop Sci*. 11 (05), 624–630. doi: 10.21475/ajcs.17.11.05.p578

Phukan, U. J., Jeena, G. S., and Shukla, R. K. (2016). WRKY Transcription Factors: Molecular Regulation and Stress Responses in Plants. *Front. Plant Sci*. 7:760. doi: 10.3389/fpls.2016.00760

Porta, H., and Rocha-Sosa, M. (2002). Plant Lipoxygenases. Physiological and Molecular Features. *Plant Physiol*. 130 (1), 15–21. doi: 10.1104/pp.010787

Povero, G., Loreti, E., Pucciariello, C., Santaniello, A., Di Tommaso, D., Di Tommaso, G., et al. (2011). Transcript Profiling of Chitosan-Treated Arabidopsis Seedlings. *J. Plant Res*. 124 (5), 619–629. doi: 10.1007/s10265-010-0399-1

Rabea, E.II, Badawy, M. E.II, Rogge, T. M., Stevens, C. V., Höfte, M., Steurbaut, W., et al. (2005). Insecticidal and Fungicidal Activity of New Synthesized Chitosan Derivatives. *Pest Manage. Sci*. 61 (10), 951–960. doi: 10.1002/ps.1085

Ramonell, K. M., Zhang, B., Ewing, R. M., Chen, Y., Xu, D., Stacey, G., et al. (2002). Microarray Analysis of Chitin Elicitation in Arabidopsis Thaliana. *Mol. Plant Pathol*. 3 (5), 301-311. doi: 10.1046/j.1364-3703.2002.00123.x

Rinaudo, M. (2006). Chitin and Chitosan: Properties and Applications. *Prog. Polymer Sci. (Oxford)* 31 (7), 603–632. doi: 10.1016/j.progpolymsci.2006.06.001

Roberts, G. A.F. (2008). Thirty Years of Progress in Chitin and Chitosan. *Prog. Chem. Appl. Chitin Deriv*. 8, 7–15.

Rogalski, M., Vieira, L. D. N., Fraga, H. P., and Guerra, M. P. (2015). Plastid Genomics in Horticultural Species: Importance and Applications for Plant Population Genetics, Evolution, and Biotechnology. *Front. Plant Sci*. 6:586. doi: 10.3389/fpls.2015.00586

Ruan, J., Zhou, Y., Zhou, M., Yan, J., Khurshid, M., Weng, W., et al. (2019). Jasmonic Acid Signaling Pathway in Plants. *Int. J. Mol. Sci*. 20 (10), 2479. doi: 10.3390/ijms20102479

Santos, A. L. W. D., Gueddari, N. E. E., Trombotto, S., Moerschbacher, B. M., Dos Santos, A. L. W., El Gueddari, N. E., et al. (2008). Partially Acetylated Chitosan Oligo- and Polymers Induce an Oxidative Burst in Suspension Cultured Cells of the Gymnosperm Araucaria Angustifolia. *Biomacromolecules* 9 (12), 3411–3415. doi: 10.1021/bm801025g

Schatz, C., Viton, C., Delair, T., Pichot, C., and Domard, A. (2003). Typical Physicochemical Behaviors of Chitosan in Aqueous Solution. *Biomacromolecules.* 4 (3), 641–648. doi: 10.1021/bm025724c

Schertl, P., and Braun, H.-P. (2014). Respiratory Electron Transfer Pathways in Plant Mitochondria. *Front. Plant Sci.* 5, 163. doi: 10.3389/fpls.2014.00163

Schmitt, F. J., Renger, G., Friedrich, T., Kreslavski, V. D., Zharmukhamedov, S. K., Los, D. A., et al. (2014). Reactive Oxygen Species: Re-Evaluation of Generation, Monitoring and Role in Stress-Signaling in Phototrophic Organisms. *Biochim. Biophys. Acta - Bioenergetics.* 837 (6), 835–848. doi: 10.1016/j.bbabio.2014.02.005

Schöttler, M. A., and Tóth, S. Z. (2014). Photosynthetic Complex Stoichiometry Dynamics in Higher Plants: Environmental Acclimation and Photosynthetic Flux Control. *Front. Plant Sci.* 5: 188:188. doi: 10.3389/fpls.2014.00188

Scott, G. J., and Suarez, V. (2012). The Rise of Asia as the Centre of Global Potato Production and Some Implications for Industry. *Potato J.* 39 (1), 1–22. doi: 10.7748/ns2012.01.26.18.1.p7241

Sharma, P., Jha, A. B., Dubey, R. S., and Pessarakli, M. (2012). Reactive Oxygen Species, Oxidative Damage, and Antioxidative Defense Mechanism in Plants under Stressful Conditions. *J. Bot.* 2012. doi: 10.1155/2012/217037

Sharp, R. (2013). A Review of the Applications of Chitin and Its Derivatives in Agriculture to Modify Plant-Microbial Interactions and Improve Crop Yields. *Agronomy* 3 (4), 757–793. doi: 10.3390/agronomy3040757

Stare, T., Ramšak, Ž., Blejec, A., Stare, K., Turnšek, N., Weckwerth, W., et al. (2015). Bimodal Dynamics of Primary Metabolism-Related Responses in Tolerant Potato-Potato Virus Y Interaction. *BMC Genomics.* 16 (1), 716. doi: 10.1186/s12864-015-1925-2

Thimm, O., Bläsing, O., Gibon, Y., Nagel, A., Meyer, S., Krüger, P., et al. (2004). MAPMAN: A User-Driven Tool to Display Genomics Data Sets onto Diagrams of Metabolic Pathways and Other Biological Processes. *Plant J.* 37 (6), 914–939. doi: 10.1111/j.1365-313X.2004.02016.x

Usadel, B., Poree, F., Nagel, A., Lohse, M., Czedik-Eysenberg, A., and Stitt, M. (2009). A Guide to Using MapMan to Visualize and Compare Omics Data in Plants: A Case Study in the Crop Species, Maize. *Plant Cell Environ.* 32 (9), 1211–1229. doi: 10.1111/j.1365-3040.2009.01978.x

Vander, P., Vårum, K. M., Domard, A., Gueddari, N. E. E., and Moerschbacher, B. M. (1998). Comparison of the Ability of Partially N-Acetylated Chitosans and Chitooligosaccharides to Elicit Resistance Reactions in Wheat Leaves. *Plant Physiol.* 118 (4), 1353–1359. doi: 10.1104/pp.118.4.1353

Vrettos, J. S., and Brudvig, G. W. (2002). "Water Oxidation Chemistry of Photosystem II," in *Philosophical Transactions of the Royal Society of London. Series B: Biological Sciences*. Eds. J. Barber and J. M. Anderson, 357 (1426), 1395–1405. doi: 10.1098/rstb.2002.1136

Wang, Y., Feng, L., Zhu, Y., Li, Y., Yan, H., and Xiang, Y. (2015). Comparative Genomic Analysis of the WRKY III Gene Family in Populus, Grape, Arabidopsis and Rice. *Biol. Direct* 10 (1), 48. doi: 10.1186/s13062-015-0076-3

Wattjes, J., Sreekumar, S., Richter, C., Cord-Landwehr, S., Singh, R., El Gueddari, N. E., et al. (2020). Patterns Matter Part 1: Chitosan Polymers with Non-Random Patterns of Acetylation. *Reactive Funct. Polymers* 151:104583. doi: 10.1016/j.reactfunctpolym.2020.104583

Wickham, H. (2011). Ggplot2. *Wiley Interdisc. Reviews: Comput. Stat* 3 (2), 180–185. doi: 10.1002/wics.147

Xoca-Orozco, L., Cuellar-Torres, E. A., González-Morales, S., Gutiérrez-Martínez, P., López-García, U., Herrera-Estrella, L., et al. (2017). Transcriptomic Analysis of Avocado Hass (Persea Americana Mill) in the Interaction System Fruit-Chitosan-Colletotrichum. *Front. Plant Sci.* 8, 956. doi: 10.3389/fpls.2017.00956

Xu, X., Pan, S., Cheng, S., Zhang, B., Mu, D., Ni, P., et al. (2011). Genome Sequence and Analysis of the Tuber Crop Potato. *Nature* 475 (7355), 189–195. doi: 10.1038/nature10158

Yamori, W., and Shikanai, T. (2016). Physiological Functions of Cyclic Electron Transport Around Photosystem I in Sustaining Photosynthesis and Plant Growth. *Annu. Rev. Plant Biol.* 67, 81–106. doi: 10.1146/annurev-arplant-043015-112002

Yao, D. C. I., Brune, D. C., and Vermaas, W. F. J. (2012). Lifetimes of Photosystem I and II Proteins in the Cyanobacterium Synechocystis Sp. PCC 6803. *FEBS Lett.* 586 (2), 169–173. doi: 10.1016/j.febslet.2011.12.010

Ye, J., Coulouris, G., Zaretskaya, I., Cutcutache, I., Rozen, S., and Madden, T. L. (2012). Primer BLAST- A Tool to Design Targer-Specific Primers for PCR. *BMC Bioinf.* 13, 134. doi: doi: 10.1186/1471-2105-13-134

Yin, H., Li, S., Zhao, X., Du, Y., and Ma, X. (2006). CDNA Microarray Analysis of Gene Expression in Brassica Napus Treated with Oligochitosan Elicitor. *Plant Physiol. Biochem.* 44 (11–12), 910–916. doi: 10.1016/j.plaphy.2006.10.002

Yoshida, K., Terashima, I., and Noguchi, K. (2011). How and Why Does Mitochondrial Respiratory Chain Respond to Light? *Plant Signaling Behav.* 6 (6), 864–866. doi: 10.4161/psb.6.6.15224

Younes, I., Sellimi, S., Rinaudo, M., Jellouli, K., and Nasri, M. (2014). Influence of Acetylation Degree and Molecular Weight of Homogeneous Chitosans on Antibacterial and Antifungal Activities. *Int. J. Food Microbiol.* 185, 57–63. doi: 10.1016/j.ijfoodmicro.2014.04.029

Zaheer, K., and Akhtar, M.H. (2016). Potato Production, Usage, and Nutrition—A Review. *Crit. Rev. Food Sci. Nutr.* 56 (5), 711–721. doi: 10.1080/10408398.2012.724479

Zuluaga, A.P., Solé, M., Lu, H., Góngora-Castillo, E., Vaillancourt, B., Coll, N., et al. (2015). Transcriptome Responses to Ralstonia Solanacearum Infection in the Roots of the Wild Potato Solanum Commersonii. *BMC Genomics.* 16 (1), 246. doi: 10.1186/s12864-015-1460-1